

SYNOPTIC PATTERNS ASSOCIATED WITH WET SEASON ONSET IN THE
TROPICAL HIGH ANDES OF SOUTHERN PERU AND BOLIVIA

A Thesis
by
TANIA KATHERINE ITA VARGAS

Submitted to the Graduate School
at Appalachian State University
in partial fulfillment of the requirements for the degree of
MASTER OF ARTS

May 2019
Department of Geography & Planning

SYNOPTIC PATTERNS ASSOCIATED WITH WET SEASON ONSET IN THE
TROPICAL HIGH ANDES OF SOUTHERN PERU AND BOLIVIA

A Thesis
by
TANIA KATHERINE ITA VARGAS
May 2019

APPROVED BY:

L. Baker Perry, Ph.D.
Chairperson, Thesis Committee

Margaret M. Sugg, Ph.D.
Member, Thesis Committee

Isabel Moreno, Ph.D.
Member, Thesis Committee

Kathleen Schroeder, Ph.D.
Chairperson, Department of Geography & Planning

Mike McKenzie, Ph.D.
Dean, Cratis D. Williams School of Graduate Studies

Copyright by Tania K. Ita Vargas 2019
All Rights Reserved

Abstract

SYNOPTIC PATTERNS ASSOCIATED WITH WET SEASON ONSET IN THE TROPICAL HIGH ANDES OF SOUTHERN PERU AND BOLIVIA

Tania K. Ita Vargas
B.S., Universidad Nacional Agraria La Molina
M.A., Appalachian State University

Chairperson: L. Baker Perry Ph.D.

In the southern Andes of Peru and Bolivia there is a clear distinction between the wet and dry season. Precipitation is one of the most relevant factors in determining glacier mass balance since the wet season onset interrupts the ablation period caused by low albedo and intense solar radiation at the end of the dry season. This study examines daily precipitation observations from 1979 to 2017 in Peru and Bolivia and identifies the wet season timing, interannual variability, and tendencies. The ERA-Interim Reanalysis (0.75° Lat/Lon - 6 hours) provide insights into the seasonal variation of wind, moisture and geopotential height related to the wet season timing over the study area. We identify spatiotemporal variations in the wet season timing mostly associated with the distance to the equator and to the Amazon basin, in which onset dates exhibits a pronounced variability. Significant trends showing the delay of the wet season onset in 0.4 to 0.8 days/year were found in the southwestern subregions, which are closely related with the occurrence of early/late wet season onset cases. A low-level northwesterly flow east of the Andes is the main feature in the lower troposphere related to the wet season onset, as well as an anticyclonic circulation in mid-

troposphere and northwesterly winds in the upper troposphere. Changes in the position and strength of these circulations are observed during early vs late wet season onset cases. This result has implications for improving seasonal precipitation predictions from tropical high Andes and in the interpretation of tropical Andean ice cores.

Acknowledgments

Completing my Master's degree is so far the most important academic accomplishment for me, which have not been possible without the absolute support of my parents, Mirtha Vargas and Jaime Ita. Especially when years ago, they supported my decision to drop up my career in Management to start a new one in Meteorology at Agrarian La Molina National University, Lima- Peru. The National Weather Service of Peru (SENAMHI-Peru) plays also an instrumental role in my personal and academic formation. I completed my internship and worked at SENAMHI for five years as a weather forecaster, during that time I had the opportunity to analyze and forecast, of course, different weather events in the country, as well travel around Peru, experiencing different climates and interacting with weather observers, their families, and local Andean communities. SENAMHI also has given me the chance to travel for the first time to the USA and participate to the International Desk Meteorology at NOAA where I got valuable training forecasting for South America. I also would like to thank my boyfriend Paul Alva, my colleague and best friend for all his emotional support, for all our daily talks, and for his guidance in personal and meteorological subjects.

I would like to thank Dr. Baker Perry, who made it possible for me to be here in the first place. Since I began with the admission process back in the fall of 2017, his guidance and support have been invaluable for me. Dr. Perry has also opened up his family's home to me for dinners and holiday celebrations. Along with the development of my thesis, Dr. Perry

always promote papers discussions, which were the base to land on my current research topic. He always motivates me and thoughtfully guides my research through every graphic, presentation, and draft of my thesis. I would also thank my committee members, Dr. Margaret Sugg, who provided insightful guidance in the statistical analysis of the thesis, and Dr. Isabel Moreno, which guidance on the formulation of the data analysis was important, as well as her knowledge in the Bolivian climate. Also thanks to my peer, Christian Barreto Schuler, who worked with me on the methodology applied in this work and helped me with processing the numerical model data. Special thanks to Joe Jonaitis, who processed all the precipitation data, simplifying this step for me, and for his sincere friendship during the time we share together in the Department of Geography and Planing.

Lastly, I would like to thank National Weather Services of Peru and Bolivia, and to the DECADE Project to provide the daily precipitation observation of southern Peru and western Bolivia used in this work. The National Science Foundation through Grant AGS-1347179 provided funding supporting this research (CAREER: Multiscale Investigation of Tropical Andean Precipitation).

Table of Contents

Abstract.....	iv
Acknowledgments.....	vi
List of Tables	ix
List of Figures	xi
Foreword.....	xiv
Introduction.....	xv
<i>Article: Synoptic Patterns Associated with Wet Season Onset in the Tropical High Andes of Southern Peru and Bolivia.....</i>	<i>1</i>
1. Introduction.....	3
2. Background and Literature Synthesis	5
3. Data and Methods	9
4. Results.....	14
5. Discussion.....	22
6. Conclusions.....	32
Appendix.....	34
References.....	35
Vita.....	69

List of Tables

Table A1. Correlation matrix perform following Pearson method among climatological wet season timing (onset, end, and duration) and geographic and topographic characteristic of each particular weather stations.	42
Table B1. Years with an early and late wet season onset in group 1 (upper and bottom in the table, respectively), showing the wet season timing, annual and wet season precipitation (mm), percentage of wet season precipitation (%), and annual and wet season precipitation anomalies (mm).	43
Table B2. Years with an early and late wet season onset in group 2 (upper and bottom in the table, respectively), showing the wet season timing, annual and wet season precipitation (mm), percentage of wet season precipitation (%), and annual and wet season precipitation anomalies (mm).	44
Table B3. Years with an early and late wet season onset in group 3 (upper and bottom in the table, respectively), showing the wet season timing, annual and wet season precipitation (mm), percentage of wet season precipitation (%), and annual and wet season precipitation anomalies (mm).	45
Table B4. Years with an early and late wet season onset in group 4 (upper and bottom in the table, respectively), showing the wet season timing, annual and wet season precipitation (mm), percentage of wet season precipitation (%), and annual and wet season precipitation anomalies (mm).	46

Table C1. Monthly precipitation (mm) (above) and monthly precipitation anomaly (mm) (below) during the very strong El Niño year (1982-83).....	47
Table C2. Monthly precipitation (mm) (above) and monthly precipitation anomaly (mm) (below) during the strong La Niña year (1988-89).....	48
Table 1. Climatological wet season timing (onset, end, and duration), annual precipitation (mm), total wet season precipitation (mm), the percentage of wet season precipitation (%), and coefficient of variation (%) of the onset, end and duration according to each group in the study area	49
Table 2. Trend Analysis, showing results from the Mann Kendall, two-sided (*) and one-sided- upward (**), Sen’s Slope and Pettitt’s test according to each group.....	50
Table 3. Wet season timing (onset, end, and duration) during the very strong El Niño year (1982-83), annual and wet season precipitation amounts and anomalies (mm) according to each group.....	51
Table 4. Wet season timing (onset, end, and duration) during the strong La Niña year (1988-89), annual and wet season precipitation amounts and anomalies (mm) according to each group.....	52

List of Figures

- Figure 1. Study area showing the location of the 43 weather stations (black dots) located above 2500 m asl, with more than 90% completeness of precipitation observations and currently operating, and the surrounding cordilleras.55
- Figure 2. Spatial distribution of the four groups, cumulative daily mean precipitation anomaly (red line) and daily mean precipitation (blue bars) in each group. The minimum and maximum points in the red line mark the onset and end dates of the wet season.....56
- Figure 3. Temporal progression of the atmospheric conditions in lower (850 hPa), middle (500 hPa) and upper (200 hPa) levels of the troposphere for the onset dates in group 4 (a, b, and c), group 2 (d, e, and f), and group 1 (g, h, and i).57
- Figure 4. The seasonal cycle of the zonal wind (ms^{-1}) in upper (a) and middle (b) levels of the troposphere averaged for the area between 18 and 12° S and 72.75 and 66.75° W. Black lines show the cumulative mean daily anomaly of this variable from 100 to 700 hPa. Colored lines represent the climatological mean daily values of the zonal wind. The pink rectangle marks the period in which wet season onset and end is establishment in all groups.....58
- Figure 5. The seasonal cycle of the meridional wind (ms^{-1}) in upper (a) and middle (b) levels of the troposphere averaged for the area between 18 and 12° S and 72.75 and 66.75° W. Black lines show the cumulative mean daily anomaly of this variable from 100 to 700 hPa. Colored lines represent the climatological mean daily values of the meridional wind.

The pink rectangle marks the period in which wet season onset and end is establishment in all groups.....59

Figure 6. The seasonal cycle of the specific humidity (gkg^{-1}) in upper (a) and middle (b) levels of the troposphere averaged for the area between 18 and 12°S and 72.75 and 66.75°W. Black lines show the cumulative mean daily anomaly of this variable from 100 to 700 hPa. Colored lines represent the climatological mean daily values of the specific humidity. The pink rectangle marks the period in which wet season onset and end is establishment in all groups.....60

Figure 7. The seasonal cycle of the sgeopotential height (gpdm) in upper (a) and middle (b) levels of the troposphere averaged for the area between 18 and 12°S and 72.75 and 66.75°W. Black lines show the cumulative mean daily anomaly of this variable from 100 to 700 mb. Colored lines represent the climatologic anomaly daily values of the geopotential height. The pink rectangle marks the period in which wet season onset and end is establishment in all groups.61

Figure 8. Mean daily precipitation (mm) and mean daily precipitation anomaly (mm) during early (a and c) and late (b and d) wet season onset cases in group 1.62

Figure 9. Mean daily precipitation (mm) and mean daily precipitation anomaly (mm) during early (a and c) and late (b and d) wet season onset cases in group 2.63

Figure 10. Mean daily precipitation (mm) and mean daily precipitation anomaly (mm) during early (a and c) and late (b and d) wet season onset cases in group 3.64

Figure 11. Mean daily precipitation (mm) and mean daily precipitation anomaly (mm) during early (a and c) and late (b and d) wet season onset cases in group 4.65

Figure 12. Monthly differences in 850 hPa between early and late wet season onset among the four groups 1 (a and b), 2 (c and d), 3 (e and f), and 4 (g and h) in October (left panels) and November (right panels). Wind in vectors (ms^{-1}), specific humidity in shaded (gkg^{-1}), and geopotential height in contour (gpdm) with solid line showing positive differences and dotted lines, negative differences.....66

Figure 12. Monthly differences in 500 hPa between early and late wet season onset among the four group 1 (a and b), 2 (c and d), 3 (e and f), and 4 (g and h) in October (left panels) and November (right panels). Wind in vectors (ms^{-1}), specific humidity in shaded (gkg^{-1}), and geopotential height in contour (gpdm) with solid line showing positive differences and dotted lines, negative differences.....67

Figure 11. Monthly differences in 200 hPa between early and late wet season onset among the four groups 1 (a nad b), 2 (c and d), 3 (e and f), and 4 (g and h) in October (left panels) and November (right panels). Wind in vectors (ms^{-1}) and geopotential height in shaded (gpdm).....68

Foreword

The main body of this thesis is formatted to the guidelines for manuscript submission to the *Journal of Applied Meteorology and Climatology*, an official journal of the American Meteorological Society.

Introduction

The tropical high Andes of southern Peru and Bolivia are part of the outer tropical region of South America, an area characterized by a well distinguished wet and dry season during the year (Kaser 2001). The annual precipitation regimen in this region is commonly associated with a wet summer and dry winter (Garreaud, et al. 2003). During the wet season, precipitation plays a relevant role in increasing water supplies that are used for domestic consumption, agriculture, hydropower, mining, and other industrial and social activities. While during the dry season, melting of glaciers located at high elevations in this area, provide fresh water used in many of the same activities. In addition, from a glaciological perspective, precipitation is one of the most relevant factors determining glaciers mass balance because it interrupts the high ablation period at the end of the dry season caused by low albedo and intense solar radiation (Francou et al 2003; Rabatel et al. 2013; Sicart et al. 2011; Wagnon et al. 1999a, b).

The study area of this work comprises Cordillera Vilcanota in Peru and Cordillera Real in Bolivia, two important glaciated areas that together account for more than 60% of all tropical glaciers in the Andes between 12 - 16°S (Rabatel et al. 2013). Since 1970s these glaciers have been experiencing an extraordinary retreat with the highest rate since the 1980s (Rabatel et al. 2013; Salzmann et al. 2013, Vuille et al. 2018), including the disappearance of small glaciers, particularly those located below 5200 m asl (Hanshaw and Bookhagen 2014). Future projections suggest that this trend will continue, changing the availability of the water resource and affecting different sectors such as hydropower, agriculture, tourism, etc., as well as ecosystems in the Andes (Vergara et al. 2007; Drenkhan et al. 2015; Kronenberg et al. 2016), increasing social and political conflicts in Andean communities (Vuille et al. 2018).

Moreover, although previous studies highlight the role of the timing and duration of the wet season as a crucial factor for glacier mass balance (Francou et al. 1995; Francou et al. 2003; Sicart et al. 2011), currently it is not fully understood when the wet season actually begins and ends or the associated synoptic patterns.

This study examines daily precipitation observations from 1979 to 2017 from 43 weather stations in southern Peru and Bolivia to identify the wet season timing following the procedure established by Liebmann and Marengo (2001), Liebmann et al. (2007), and Dunning et al. (2016). Secondary objectives in this work are the examination of the interannual variability, tendencies, and the analysis of two ENSO events, the very strong El Niño (1982-83) and the strong La Niña (1988-89). Atmospheric fields from the ERA-Interim Reanalysis (0.75° Lat/Lon - 6 hours) are analyzed in the same period (from 1979 to 2017) to provide insights into the seasonal variation of zonal and meridional wind, moisture content of the air and geopotential height related to the wet season timing over the study area.

Results from the precipitation data analysis reveal spatiotemporal differences in the wet season timing across the study area, with an early wet season onset in sites adjacent to the Amazon basin and late wet season onset in areas located close to the Pacific basin. Additionally, within the wet season timing, the onset dates show a high interannual variability, reflected in the 37-day period in which the wet season is established throughout the study area, contrary to the end dates that occurs almost at the same time across the study area. Over the period analyzed, the wet season onset was strongly correlated with the wet season duration. In this sense, most of the cases of early wet season onset are associated with a long wet season. Statistically significant positive trends in the onset dates were found in sites southwest to the Titicaca Lake, indicating a delay in the wet season onset in the range of

0.4 and 0.8 days per year. Moreover, detected cases of early and late wet season onset are commonly associated with positive and negative annual and wet season precipitation anomalies. The comparison of El Niño and La Niña cases show positive and negative precipitation anomalies, respectively, in the month in which the wet season onset is established. The analysis of the reanalysis data reveal that a low-level northwesterly flow in lower troposphere is the main feature related to the establishment of the wet season onset in the study area, while in middle troposphere a eastward movement of an anticyclonic circulation favors the moisture transport from the Amazon basin into the high Andes of the southern Peru and Bolivia. In the upper troposphere, northwesterly flow, with velocities below to the annual mean moves to the south with the Bolivian high, a anticyclonic circulation, while divergence to support precipitation is generated by the interaction of the northwesterly flow and the Bolivian High. Changes in the position and strength of these circulations are observed during early vs late wet season onset cases.

Findings from this study will help to complete our understanding on the seasonality of precipitation in this region. In addition, results can be used to improve short and mid-range forecast of the wet season timing in order to develop and implement contingency plans when forecast conditions are far from normal. Special attention deserve the areas in which a delay trend were found, since this trend would considerably affect the availability of water in the future. We also believe that these results have implications for improving the interpretation of tropical Andean ice cores.

In the development of this project, Tania Ita took a leading role in its formulation. She assisted with the collection of precipitation and reanalysis data and completed all of the data analysis, figure generation, writing, and formatting of this manuscript. Dr. Baker Perry

provided invaluable guidance and knowledge, contributing to ideas discussed in this study, and providing financial and emotional support. Dr. Magaret Sugg, contributed with her expertise in statistical analysis applied in this work and provided different perspectives on the data analysis. Dr. Isabel Moreno, provided guidance on the formulation of the data analysis and her knowledge in the Bolivian climate was relevant for this work. Christian Barreto provided valuable help in the analysis of precipitation and reanalysis datasets.

1 **Synoptic Patterns Associated with Wet Season Onset in the Tropical High**

2 **Andes of Southern Peru and Bolivia**

3 Tania K. Ita Vargas, L. Baker Perry* and Margaret M. Sugg

4 *Appalachian State University, Boone, North Carolina, USA*

5 Isabel Moreno

6 *Universidad Mayor de San Andrés, La Paz, Bolivia*

7 Christian Barreto Schuler

8 *York University, Toronto, ON, Canada*

9 *Corresponding author address: Dr. L. Baker Perry, Dept. of Geography and Planning, Ap-
10 palachian State University, 572 Rivers Street, RSW 323C, Boone, NC 28608

11 E-mail: perrylb@appstate.edu

ABSTRACT

12 In the southern Andes of Peru and Bolivia there is a clear distinction be-
13 tween the wet and dry season. Precipitation is one of the most relevant factors
14 in determining glacier mass balance since the wet season onset interrupts the
15 ablation period caused by low albedo and intense solar radiation at the end
16 of the dry season. This study examines daily precipitation observations from
17 1979 to 2017 in Peru and Bolivia and identifies the wet season timing, interan-
18 nual variability, and tendencies. The ERA-Interim Reanalysis (0.75° Lat/Lon
19 - 6 hours) provide insights into the seasonal variation of wind, moisture and
20 geopotential height related to the wet season timing over the study area. We
21 identify spatiotemporal variations in the wet season timing mostly associated
22 with the distance to the equator and to the Amazon basin, in which onset dates
23 exhibits a pronounced variability. Significant trends showing the delay of the
24 wet season onset in 0.4 to 0.8 days/year were found in the southwestern subre-
25 gions, which are closely related with the occurrence of early/late wet season
26 onset cases. A low-level northwesterly flow east of the Andes is the main
27 feature in the lower troposphere related to the wet season onset, as well as
28 an anticyclonic circulation in mid-troposphere and northwesterly winds in the
29 upper troposphere. Changes in the position and strength of these circulations
30 are observed during early vs late wet season onset cases. This result has im-
31 plications for improving seasonal precipitation predictions from tropical high
32 Andes and in the interpretation of tropical Andean ice cores.

33 **1. Introduction**

34 The Cordillera Vilcanota and Cordillera Real are two very important glacierized areas located in
35 the tropical high Andes of southern Peru and Bolivia. Together, they account for more than 60%
36 of all tropical glaciers in the Andes between 12 - 16° S (Rabatel et al. 2013). As part of the outer
37 tropical Andes, this region is characterized by an annual precipitation regimen, which is associated
38 with a well distinguished wet summer and dry winter (Garreaud et al. 2003). During the wet
39 season, precipitation is the primary input for domestic consumption, agriculture, hydropower, and
40 other industrial activities. During the dry season, however, glacier runoff provides fresh water used
41 in different socioeconomic activities. Moreover, from a glaciological perspective, precipitation is
42 one of the most relevant factors determining the mass balance of glaciers because it interrupts the
43 high ablation period at the end of the dry season caused by low albedo and intense solar radiation
44 (Wagnon et al. 1999a,b; Francou et al. 2003; Sicart et al. 2011; Rabatel et al. 2013).

45 Since the 1970s, glaciers in the outer tropical Andes have been experiencing an exceptional
46 retreat, the highest rate since the 1980s (Rabatel et al. 2013; Salzmann et al. 2013; Vuille et al.
47 2018). Small glaciers have disappeared in this period, particularly those located below 5200 m asl
48 (Hanshaw and Bookhagen 2014). Future climate projections suggest that this tendency will change
49 the availability of the water resource affecting different sectors such as hydropower, agriculture,
50 tourism, etc., as well as ecosystems in the Andes (Vergara et al. 2007; Drenkhan et al. 2015;
51 Kronenberg et al. 2016; Schauwecker et al. 2017). Social and political conflicts are likely to
52 increase, not only due to water availability, but also due to conflicting cultural beliefs of Andean
53 communities about glaciers (Vuille et al. 2018). Although previous studies highlight the role of
54 the timing and duration of the wet season as a crucial factor for glacier mass balance (Francou

55 et al. 1995, 2003; Sicart et al. 2011), there is no objective method for determining beginning/end
56 of the wet season or the associated synoptic patterns.

57 By using daily precipitation data from weather stations located at high elevations in the southern
58 Andes of Peru and Bolivia ERA-Interim Reanalysis datasets, this study investigates synoptic-scale
59 atmospheric circulation associated with wet season onset in the outer tropical Andes. Secondary
60 objectives include 1.) the determination of the interannual variability of the wet season timing; 2.)
61 the identification of trends in the onset dates; 3.) the evaluation of early versus late wet season
62 onsets; and 4.) the examination of the wet season timing during one El Niño and La Niña event.
63 The analysis of the ERA-Interim Reanalysis will provide insight into the atmospheric circulations
64 over the outer tropical Andes associated with the wet season onset and cases of early/late wet
65 season onset.

66 The remainder of the manuscript is structured as follows: in section 2, a synthesis about the
67 current understanding of the atmospheric mechanisms that control precipitation in different time
68 scales is presented; section 3 describes the data and the methods used to assess the wet season tim-
69 ing and its implementation, as well as the statistical tests used to assess the interannual variability,
70 trends and comparison among the data– this section also describes the computational process per-
71 formed with ERA-Interim Reanalysis; in section 4 and 5, the results and their implications are
72 presented and discussed, respectively; finally, section 6 summarizes the findings and presents the
73 future direction of this work.

74 **2. Background and Literature Synthesis**

75 *a. The seasonal and sub-seasonal cycle of precipitation in the outer tropical Andes*

76 The seasonal cycle of wet summer and dry winter in the outer Andes of South America have been
77 widely described in many studies (Vuille 1999; Lenters and Cook 1999; Garreaud et al. 2003).
78 Perry et al. (2013) found that between 2004 and 2010 in Cordillera Vilcanota (southern Peru)
79 the annual mean of precipitation is 697 mm, with more than 50% of the annual mean occurring
80 during the austral summer (December, January, and February) and only 1-2% of the annual mean
81 falling during the austral winter (June, July, and August). Moreover, Andrade (2018) found that
82 over southern Peru and western Bolivia 80% of the annual precipitation falls between November
83 and April in a period called the extended wet season, while the remaining 20% occurs between
84 May and October, called the extended dry season. This study also revealed that in the western
85 region almost 100% of precipitation occurs during the extended wet season. In addition, from a
86 glaciological perspective, some authors also define a transition season between the dry and the
87 wet season, in which precipitation increases gradually until the height of the wet season, when the
88 amount and frequency of precipitation is highest (Kaser 2001; Francou et al. 2003; Sicart et al.
89 2011; Rabatel et al. 2013). Regarding that, Andrade (2018) described that the transition from the
90 dry to wet season occurs in two months (October and November), while the transition to the dry
91 season occurs just in one month (April). Indeed, this pronounced seasonal cycle of rainfall can
92 also be observed at the continental scale and it seems to be closely related with the South America
93 Monsoon System (Garreaud et al. 2009).

94 During the austral winter (JJA), westerly winds prevail in the middle and upper troposphere over
95 the Altiplano, consequently with the north most position of the subtropical jet stream. Near-surface
96 moisture is low, with values below 2 gkg^{-1} mixing ratio that cannot support convective rainfall

97 (Garreaud et al. 2003). Nevertheless, precipitation can occur in this season, which is associated
98 with upper-level mid-latitude disturbances moving abnormally north of their mean paths, such
99 as cut-offs lows and deep troughs. In addition, cold fronts that penetrate the Altiplano are also
100 responsible for precipitation in this season (Vuille 1999; Garreaud et al. 2003). During austral
101 spring (SON), these patterns gradually change due to the southward shift of the peak insolation.
102 By late spring, clear variations are observed in all levels of the troposphere, such as the southward
103 shifting of the subtropical jet stream and the enhance in convective precipitation in the central part
104 of the continent and southern Amazon basin (Garreaud et al. 2003).

105 During the austral summer (DJF), the release of latent heat due to convection in the Amazon
106 basin leads to the development of the Bolivian high, an upper-level anticyclone circulation center
107 approximately at 15° S and 65° W during the summer, also accompanied by a cyclonic circulation
108 downstream over the northeast of Brazil (Lenters and Cook 1995, 1999). The establishment of this
109 system, along with the southward displacement of the subtropical jet stream, allow the southward
110 expansion of the equatorial belt of easterly winds that persist in middle and upper levels to the
111 troposphere in this season transport moist air from the Amazon basin into the Altiplano and thus
112 enabling the development of precipitation (Garreaud et al. 2003). In addition, trajectory analyses
113 highlight the importance of the low-level moisture transport into the Cordillera Vilcanota of Peru,
114 and Cordillera Real of Bolivia by a northwesterly flow east of the Andes during precipitation events
115 in this region (Perry et al. 2013, 2017). Indeed, during the austral summer, a deep continental low
116 lays over the Chaco region forcing winds, east to the Andes, turn southward while exhibiting a
117 low-level jet structure (Garreaud et al. 2009). Moreover, Chavez and Takahashi (2017) suggest a
118 close relation between the nocturnal precipitation in this region and the peak of the SALLJ, which
119 also occurs during the night and more frequently with a maximum extension along the eastern
120 flank of the Andes during the summer (Nogués-Paegle and Mo 1997; Marengo et al. 2004).

121 In the wet season, precipitation in the outer tropical Andes is overall episodic; rainy days are
122 grouped in a series of about one to two weeks and separated by dry periods of similar durations
123 (Garreaud et al. 2003; Andrade 2018; Guy et al. 2019). Two main synoptic circulations over the
124 Altiplano related with the wet episodes are stronger than average easterly winds in the middle
125 and upper troposphere, and a southward displacement of the Bolivian high (Vuille 1999; Garreaud
126 et al. 2003). Additionally, Lenters and Cook (1999) describe three synoptic circulations related to
127 intraseasonal wet periods in the Altiplano. The first synoptic circulation is a low pressure located
128 southeast of the Altiplano in the form of El Chaco low or a propagating extratropical cyclone
129 further south. The second synoptic circulation is northerly winds along the northern central Andes
130 and along the eastern flank of a cold core low located in southeastern South America. Finally, the
131 third synoptic circulation is the westward enhancement of the South American Convergence Zone
132 SACZ (Lenters and Cook 1999).

133 The daily cycle of precipitation is commonly bimodal, with two peaks, one during the after-
134 noon around 16:00 LST and the other one around midnight, local time (Perry et al. 2013, 2017;
135 Chavez and Takahashi 2017; Junquas et al. 2017; Endries et al. 2018). The character of afternoon
136 precipitation is the primary convective product of the thermal heating of the Andes. Nighttime
137 precipitation is generally stratiform (Perry et al. 2017; Chavez and Takahashi 2017; Endries et al.
138 2018) and the meteorological forcing seems to be related with a mesoscale convective system lo-
139 cated in a downslope region in the Peruvian jungle around 700 m asl, with its stratiform component
140 extending upslope in the Peruvian mountains. Moreover, these convective systems are stronger un-
141 der SALLJ conditions, whose maximum peak also occurs during the night (Chavez and Takahashi
142 2017; Junquas et al. 2017).

143 *b. Impact of ENSO on the wet season in the outer tropical Andes*

144 In South America, ENSO is the principal mode of interannual variability of summer precipita-
145 tion (Zhou and Lau 2001), generating different effects throughout the continent. Lenters and Cook
146 (1999) found in the Altiplano region dry conditions during the 1987 El Niño summer, associated
147 with a weakened and northward displacement of the Bolivian high, and the presence of cold and
148 dry southerly flow in lower levels of the troposphere east of the Andes. Vuille (1999) also found
149 a deficit of precipitation in the Nevado Sajama region during El Niño and precipitation above
150 the normal conditions during La Niña and in summers following El Niño years, despite the fact
151 that these changes in precipitation were statistically insignificant at 95% level. Meanwhile, Gar-
152 reaud and Aceituno (2001) indicated that rainfall anomalies in the Altiplano during ENSO events
153 strongly depend on the locations of zonal wind anomalies that are associated with a warming or
154 cooling troposphere during the warm and cold phase of ENSO, respectively. Recent studies, also
155 found differences in the spatial distribution of precipitation in southern mountains of Peru and
156 Bolivia, showing precipitation amounts above the average during El Niño and amounts below the
157 average during La Niña years in Cusco, Peru, and negative precipitation anomalies during El Niño
158 and La Niña in El Alto, Bolivia (Perry et al. 2013, 2017).

159 From a glaciological point of view, on interannual timescales, ENSO plays an important role
160 in the evolution of tropical glaciers. Francou et al. (2003) found that changes in the Chacaltaya
161 glacier were controlled by SST anomalies in the eastern equatorial Pacific Ocean (Niño 1+2 area).
162 Additionally, Rabatel et al. (2013) concluded that the variability of the tropical Pacific SST is
163 the main factor controlling the interannual variability of glacier mass loss. Moreover, in a close
164 analysis of the 1991-92 El Niño event in the Zongo glacier, Bolivia, Francou et al. (1995) found
165 accelerating melting conditions in the ablation area due high temperatures and low precipitation

166 during the warm season. Then, during the 1997-98 strong El Niño event, the Zongo glacier again
167 experienced a deficit in precipitation, increase in temperature, and a strongly negative mass bal-
168 ance (Wagnon et al. 2001). After a detailed evaluation of radiative fluxes, Wagnon et al. (2001)
169 concluded that the main factor in the highly negative glacier mass balance was the substantial
170 increase in net all-wave radiation, which was three times higher than the previous years.

171 **3. Data set and Methods**

172 *a. Data sets*

173 The study area of this research was in southern Peru and western Bolivia, part of the outer Trop-
174 ical Andes of South America (Fig. 1). The National Weather Services of Peru (SENAMHI-Peru)
175 and Bolivia (SENAMHI-Bolivia), and the project Data on Climate and Extreme Weather for the
176 Central Andes (DECADE) (Andrade 2018; Hunziker et al. 2018) provided daily precipitation data
177 from 43 weather stations located at high elevations from 1979 to 2017 (Fig. 1). For the analysis,
178 only weather stations with more than 90% of complete information were used; also, only operating
179 weather stations were used to ensure future evaluation of the evolution of the wet season timing
180 in the region. In addition, the mean product of the Global Multi-resolution Terrain Elevation Data
181 2010 (GMTED2010), with a spatial resolution of 0.0020833333 decimal degrees (Danielson and
182 Gesch 2011) was used for the South American region to obtain variables, such as slope and aspect
183 in the location of each weather stations. Finally, the Era-Interim Reanalysis, a global atmospheric
184 reanalysis dataset with 0.75° latitude/longitude horizontal resolution and 6 hours of temporal res-
185 olution (Dee et al. 2011) were used to assess the synoptic conditions associated with wet season
186 timing.

187 *b. Method*

188 To determine the timing of the wet season, we adapted the method used by Liebmann and
189 Marengo (2001); Liebmann et al. (2007) in South America and more recently applied in Africa
190 by Dunning et al. (2016). For the identification of the onset and end dates of the wet season in
191 an annual precipitation regimen, the cumulative daily mean rainfall anomaly was calculated $C(d)$.
192 The calculation starts with the climatological mean rainfall, Q_i , where i goes from 1 January to
193 31 December. Then, the climatological daily mean rainfall, \bar{Q} , is computed. Thus, the cumulative
194 daily mean rainfall anomaly on day d , $C(d)$, is found:

$$C(d) = \sum_{i=1Jan}^d Q_i - \bar{Q} \quad (1)$$

195 In the equation, $C(d)$ is calculated for each day of the calendar year from 1 January to 31 Decem-
196 ber, however, Liebmann et al. (2007) states that the calculation can be started at any time of the
197 year, but in practice it is started 10 days prior to the beginning of the driest month and is continued
198 for a year. Thus, the onset and end dates are determined by finding the minimum and maximum
199 values of the cumulative daily mean rainfall anomaly curve, respectively, which increases when
200 the daily precipitation is above the climatological daily mean rainfall, and decreases when it is
201 below the climatological daily mean rainfall (Dunning et al. 2016). Additionally, as a previous
202 step to this calculation, it was necessary to adjust the data. This process included the construction
203 of the hydrologic years that span from July 1 to June 30 of the next year, and the elimination of
204 February 29 according to Liebmann and Marengo (2001). Thus, the calculation of the cumulative
205 daily rainfall mean anomaly starts on July 1, instead of on January 1. Moreover, henceforth we
206 will use the term precipitation instead of rainfall since both solid and liquid precipitation types can
207 occur in the study area.

208 Given that wet season timing in the region was variable across the study area, groups were
209 identified following a weighing process and a quantile classification. A first step involved the
210 examination of the distribution of the climatological onset, end, and duration of the wet season,
211 together with the latitude, longitude, elevation, slope, and aspect by using the Shapiro-Wilk test.
212 The second step was assessing the the strength of the relationship among these variables. The
213 purpose of correlating the wet season timing with the geographic variables and topographic char-
214 acteristic of each precipitation site was to identify relationships to help in the identification of
215 similar spatiotemporal patterns. Latitude, longitude, and elevation information were provided by
216 SENAMHI-Peru, SENAMHI-Bolivia and DECADE Project, while slope and aspect values were
217 calculated from the terrain elevation model for the location of each weather station. Correlation
218 matrix were constructed to all variables using the Pearson or Kendall correlation coefficient, which
219 was determined based on the normality of the data. In both cases, the duration of the wet season
220 showed the highest correlation values with the geographic and topographic variables than the onset
221 and end dates (Table A1), and since the duration of the wet season is a summary measure of the
222 onset and end dates, its correlation values were used in the weighting process. The geographic
223 and topographic variables were standardized using the z-scores before performing the weighting
224 process using the correlation values of both the Pearson and Kendall methods, separately, in which
225 the sign of the correlation was omitted given that in this step only the magnitude of the correla-
226 tion is important, not the direction. Finally, the number of groups was found following quantile
227 classification and mapped to evaluate the spatial distribution.

228 To determine the number of groups, as well as the best option in the weighting process (Pear-
229 son or Kendall methods) the spatial distribution and a sensitivity analysis, which included the
230 evaluation of wet season timing and wet season precipitation, as well as the trend analysis us-
231 ing the Mann-Kendall, Sen's slope and Pettitt's test, was done to examine these variables among

232 the groups. The sensitivity analysis revealed that by reducing the number of groups from four to
233 three, the wet season timing and precipitation were more homogeneous among the groups; like-
234 wise, trends found in the four-group classification were not observed when applying a three-group
235 classification. Therefore, we decided to use the Pearson correlation and the four-group classifica-
236 tion, which achieve a better detail of the characteristics of the study region. Once the groups were
237 determined, the mean annual precipitation (mm), wet season precipitation (mm), the percentage
238 of precipitation during the wet season (%), and coefficient of variation CV (%), were computed
239 for each group.

240 In a second stage, the climatic wet season timing was found for each group. Then, the onset
241 and end dates were identified for each individual hydrologic year, using the mean precipitation of
242 each group. The high year-to-year variation in precipitation amount complicates the identification
243 of the minimum and maximum point in the entire cumulative curve at once. Thus, the onset date
244 was found between the first day of the hydrologic year (July 1) and the last day, in which the
245 cumulative daily mean precipitation anomaly of a particular group still presents negative values.
246 The end dates were found between the first day, in which the cumulative daily mean precipitation
247 anomaly of a particular region presented a positive value, and the last day of the hydrologic year
248 (June 30). With his yearly information, early and late cases of wet season onset were identified
249 and taken into account thresholds, which were determined by the bottom and top quartile of the
250 onset dates for each group, respectively.

251 The trend analysis was carried out for each group from 1979-80 to 2016-17 hydrologic years,
252 with the data obtained in the second stage of the determination of the wet season timing. The
253 Mann-Kendall test is widely used to asses hydro-meteorological time series since it is more suit-
254 able for non-normal distributed data and it is less sensitive to outliers (Hamed and Raos 1998;
255 Yue et al. 2002). Nevertheless, it was necessary to first examine the assumptions of the Mann-

256 Kendall test; in this sense, the serial correlation among the onset dates was evaluated using the
257 Autocorrelation Function (ACF) and Partial Autocorrelation Function (Partial ACF). Since no se-
258 rial correlation was found, the Mann Kendall test was applied; also, the Sens slope and Pettitts test
259 were used to add more information to the traditional trend analysis, being able to detect the slope
260 of the trend line (the magnitude) and a possible break point in the time series, respectively. All
261 tests previously mention before are available in the trend package in R (Pohlert 2018).

262 To investigate the synoptic conditions associated with the wet season timing, particularly, the
263 wet season onset, we constructed a daily climatology of the ERA-Interim Reanalysis using the
264 4-time daily products of this reanalysis. Variables analyzed included zonal and meridional wind
265 (ms^{-1}), specific humidity (gkg^{-1}), and geopotential (m^2s^{-2}). The daily climatology also follows
266 the hydrologic year and has the same period as the precipitation data from 1979-80 to 2016-17.
267 Then, the seasonality of these variables was examined using the same equation we used with
268 precipitation data. This computation was done by averaging grid cells of the reanalysis dataset
269 between 18 and 12° S and 72.75 to 66.75° W, we include all the mandatory levels in this analysis,
270 however, the low level was not considered. To assess the synoptic conditions during the evolution
271 of the wet season onset and during cases of early and late wet season onset, daily and monthly
272 composites were done, particularly for the early versus late cases. Differences between those
273 cases (early minus late) were computed for lower (850 hPa), middle (500 hPa), and upper (200
274 hPa) levels of the troposphere. Finally, we compare the behavior of the wet season timing during
275 two ENSO events, the very strong El Niño of 1982-83 and the strong La Niño of 1988-89. Results
276 obtained in the second stage of our analysis were used for this purpose; in addition, for a close
277 analysis, monthly precipitation and monthly precipitation anomalies, based on the 1979-2017 time
278 period, were calculated during the 1982-83 and 1988-98 hydrologic year.

279 **4. Results**

280 *a. Climatological wet season timing*

281 Along the study area, four groups were identified Fig. 2. The spatial distribution of these reveals
282 an NW-SE orientation, where groups 1 and 2 are located to the southwest of the Titicaca Lake,
283 over the Peruvian and Bolivian Altiplano and close to the Pacific basin. Groups 3 and 4 are situated
284 northeast to the Titicaca Lake, nearby to Cordilleras Vilcanota and Real and to the Amazon basin.
285 The daily evolution of precipitation in each group (Fig. 2) shows a gradual increase in precipitation
286 amounts during the transition from the dry to the wet season. However, the transition from wet to
287 the dry season occurs in a short time period for all groups. There also exist differences in daily
288 precipitation amount along the year, with group 1 showing the lowest precipitation values among
289 the others.

290 Additionally, differences are shown in Table 1, in which we observe a gradual progression of
291 the onset dates that initiate first in the group 4 on 24 October, then progress to groups 3 and 2
292 on 12 and 13 November, respectively, and lastly it occurs on group 1 on 11 November. The end
293 of the wet season takes place between 5 and 11 April, in which the end of the wet season occurs
294 first in the group 1 and gradually occurs in the group 4 in a seven-day period. Hence, due to
295 this opposite behavior in the occurrence of the onset and end dates, the longest duration of the
296 wet season occurs in group 1 with 170 days, and the shortest in group 4 with 127 days. The
297 amount of annual precipitation reveals an increase from groups 1 to 3 and then a decrease in group
298 4; however, the total amount of precipitation during the wet season increases from group 1 to
299 group 4. The percentage of precipitation during the wet season reveals slight differences between
300 groups 2 and 3, still showing an upward tendency from groups 1 to 4. The variability among
301 the wet season timing was assessed through the coefficient of variation (CV), revealing that there

302 exist more variability in the duration of the wet season in the onset dates than in the end dates.
303 Regarding the onset, this is reflected in the long period in which the wet season onset occurs,
304 37 days between the onset in group 1 and 4. Moreover, since the duration of the wet season is
305 more strongly correlated to the onset (Table A1), the CV is even higher for the duration given
306 that this also depends on the end dates variability. The end dates have a lower variability, related
307 in the seven day period between the occurrences of this from groups 1 to 4. CV values tend to
308 decrease from groups 1 to 4 for the end dates and wet season duration, while the opposite behavior
309 is observed for the onset dates, except for groups 4 that shows the second lower value.

310 *b. The relationship between wet season timing and atmospheric circulations*

311 During the onset date of groups 1, on October 24, a northwesterly flow in 850 hPa (Fig. 3a)
312 extent east to the Andes from the central jungle of Peru to southern Bolivia, then, the flux turned
313 to the east over Paraguay and central Argentina. This low-level flux reaches its highest velocities
314 over central Bolivia, Paraguay, and Argentina. By the time of the onset date of group 3, on 13
315 November (Fig. 3d) (the onset in group 2 occurs just one day before), the low-level flux became
316 more elongated, particularly in its northward site, showing high velocities along the jungle of
317 Colombia and Peru and a decrease in wind speed over Bolivia and Paraguay. Lastly, at the moment
318 of the onset date of group 4 (Fig. 3g) the northwesterly flux shows a notable increase of the wind
319 speed in the north of the continent, over Colombia and Peru, and again over Bolivia, while a
320 decrease is observed over Argentina. The Atlantic high-pressure winds show a weakening with
321 the temporal progression of wet season onset, which is related to the confinement of the moisture
322 content in the center of the continent during the onset date of group 1. The evolution of this low-
323 level flow is closely associated with the southwest displacement of the northern trade winds that
324 allow the increase of wind speed, particularly over the Colombia jungle and favoring the southward

325 displacement of moisture toward southern latitudes (Nogués-Paegle and Mo 1997). The decrease
326 in velocities over Argentina can be linked to the displacement of the convection to the north, since
327 the exit region of the low-level jet is related with convective activity (Nogués-Paegle and Mo 1997;
328 Marengo et al. 2004).

329 In 500 hPa, an anticyclonic circulation shifts to the west, toward the Pacific ocean, as the winds
330 at latitudes south of the 20° S slow down since the occurrence of the onset date in group 1 (Fig.
331 3b) until the onset date in group 4 (Fig. 3h). This anticyclonic circulation is indicated to be part of
332 the Bolivian high by Vuille (1999), and from the dry to the wet season it moves to the southwest
333 to finally reach a location between south Bolivia and northern Argentina around January (Gilford
334 et al. 1991). The movement of the 500 hPa circulation favors southeasterly winds over the study
335 area, that are intensified toward the onset date in group 4, generating at the same time a major
336 moisture influx. In upper levels of the troposphere (200 hPa), a gradual increase in geopotential
337 height values, as well as an NW-SE expansion occurs (Fig. 3c, f, and i), associated with the devel-
338 opment of the Bolivian high. However, the southward shift of this system is slight compared to its
339 position over central Bolivia during wet periods within the wet season (Vuille 1999). Moreover,
340 the northwesterly winds over the Pacific Ocean prevail from 24 October to 30 November despite
341 the presence of the Bolivian high.

342 *c. The seasonal cycle of wind, moisture content, and geopotential height over the central Andes*

343 The analysis of the seasonal cycle of atmospheric variables from the ERA-Interim reanalysis
344 reveals differences in the temporal evolution of zonal and meridional wind, specific humidity
345 and geopotential height in middle and upper levels of the troposphere over the study. The zonal
346 wind has a positive annual mean (from the west) in all levels analyzed. The detection of the
347 maximum and minimum points in the cumulative curve (minimum and maximum point for the

348 other variables) marks the period associated with the onset and end of the wet season, respectively.
349 Among 400 and 100 hPa (Fig. 4a), these points occur almost at the same time, between 14 and
350 15 October for the maximum point, and between 15 and 17 April for the minimum point. By the
351 time the maximum point occurs, the zonal wind maintains its direction from the west and its speed
352 around 4, 10, 7, and 3 $m s^{-1}$ in 100, 200, 300 and 400 hPa, respectively, which are close to their
353 annual mean. When the minimum point occurs, the zonal wind again reveals a direction from the
354 west, while velocities are similar to the ones before. Moreover, during the establishment of the
355 wet season in all groups, westerly winds prevail, with magnitude lower than the annual mean of
356 each particular level. Therefore, at the beginning of the wet season, the presence of easterly winds
357 is not necessary, but there is a decrease in wind speed. After that, the wind speed decreases and
358 eventually it comes from the east but not during the entire wet season. In middle levels of the
359 troposphere (Fig. 4b), the behavior of the zonal wind is quite similar to the one in upper levels;
360 nevertheless, the seasonality is barely noticeable in 700 hPa, since at this level wind direction does
361 not considerably change along the year keeping its westerly direction. Principally, in 500 hPa,
362 before the establishment of the wet season, a change in wind direction occurs, and easterly winds
363 prevail until the end of the wet season.

364 Contrary to what we found analyzing the zonal wind, the seasonality of the meridional wind
365 in upper levels (Fig. 5a) reveals a different pattern of two cycles of decreasing and increasing
366 magnitude of southerly winds that prevails during the year between 300 and 100 hPa. While in
367 the 400 hPa level, a slight change in wind direction is observed, following the pattern of middle
368 level winds. Nevertheless, by the time the wet season is established an increase in the magnitude
369 is observed. In 400 hPa, the minimum point occurs on 16 October and the maximum on 30 March.
370 Contrary to what was stated in the zonal wind, the cumulative curve here shows first a decrease
371 and then an increase; this difference is due to the direction of the wind. In 600 and 500 hPa (Fig.

372 5b), the seasonality is clearer due to the change in wind direction by the time of the wet season.
373 Despite this, change does not last the entire wet season. The minimum point in the cumulative
374 curve occurs on 30 September and 3 October, in the 500 and 600 hPa level, respectively, before
375 the wet season onset in all subregions. The maximum point in this curve occurs on March 26 and
376 April 14, for the same levels. In 700 hPa, like the 100, 200 and 300 hPa, the change in wind speed
377 along the year is slight.

378 Specific humidity (Fig. 6) shows a clear evolution in all levels analyzed. However, it is hard to
379 distinguish in 100 and 200 hPa because of the low moisture content in these levels. The annual
380 mean of specific humidity ranges from 0.003 gkg^{-1} in 100 hPa to 6.7 gkg^{-1} in 700 hPa. Similar
381 to the zonal wind, the minimum and maximum point in the cumulative curve occurs when the
382 mean daily specific humidity reaches values near annual mean in each specific level. Dates of
383 the minimum point in the cumulative curve occur almost at the same time in all levels, with the
384 exception of the 100 hPa. This is between 17 and 22 October, while the maximum point occurs in
385 a 15 days range, between 12 and 27 April.

386 The seasonal cycle of geopotential height (Fig. 7) reveals a different behavior in the cumulative
387 curve, showing a decrease toward the wet season onset and an increase toward the end of the wet
388 season in upper levels (Fig. 7a); the behavior of the cumulative curve shows the opposite behavior
389 in middle levels (Fig. 7b). Like the specific humidity and zonal wind, the minimum and maximum
390 points in the curve are associated with the annual mean values in each level. Dates related to
391 the wet season onset occur in a wide range in middle and upper levels. In the upper level, dates
392 associated with the wet season onset are 20 and 22 October, in 200 and 300 hPa, respectively. It
393 occurs later on 10 and 21 November, in 100 and 400 hPa. In middle levels, dates are 30 September
394 and 10 October, in 700 and 600 hPa. Dates related with the end of the wet season are late in May
395 and early June in upper levels and between February and March in middle levels.

396 *d. The character of early and late wet season onset*

397 After identifying years in which an early and late wet season occurs in each group, we found that
398 since 1979, an average of eight cases of early wet season onset have occurred, while the average of
399 late-onset cases increased to nine. Years characterized by an early wet season onset (Table B1-B4)
400 reveal different behaviors in the occurrence of an early or a late wet season end; however, since
401 the onset is strongly correlated with the wet season duration, in most of the cases, early onsets are
402 associated with a long wet season. In addition, both the total amount of annual and wet season
403 precipitation mostly present positive anomalies during early onset cases. On the other hand, years
404 that present a late wet season onset (Table B1-B4) do not present a clear association with early
405 or late end of the wet season; however, the duration of the wet season is shorter compared to its
406 climatic values. The total annual and wet season precipitation decreases for most of the cases.
407 This decrease is observable in the percentage of precipitation during the wet season. After this
408 comparison, it was clear that an early or late wet season onset does not mean an early or late
409 wet season end. The role of topography is also pointed out in this analysis since that in any
410 given year, groups can present a case of an early or late wet season onset at the same time. In
411 this sense, it is possible to present an event of early onset in a group and a late case in another.
412 Even though this behavior is not common during the period analyzed. The inspection of the daily
413 mean precipitation during early and late wet season onsets reveals differences in the temporal
414 distributions of precipitation in each group (Fig. 8, 9, 10, 11).

415 *e. Synoptic conditions associated with early and late wet season onset*

416 Atmospheric circulation in 850 hPa (Fig. 12) reveals that the main difference between cases of
417 early and late wet season onset is related to a stronger low-level northwesterly flow over Bolivia,
418 Paraguay and Argentina that in turn is associated with southward moisture transport. Other at-

419 mospheric features include the presence of low pressure over northern Argentina and Paraguay,
420 and a high-pressure east of this system, on the Atlantic ocean. From October to November, these
421 systems appear more intense, particularly, the high-pressure system. Although these systems are
422 common for the four groups, a better configuration, as well as larger differences in the moisture
423 content and wind speed are observed for the group 1. The more intense low-level flow is supported
424 by the development of a low pressure over the continent. In addition, the high-pressure system also
425 helps to transport moisture content to southern latitudes, and as a result, a contrast is observed in
426 the continent, with dry conditions on the northern part and moist conditions in the southern part of
427 South America.

428 In mid-troposphere (Fig. 13) a pattern of weakening westerly winds between 15 and 25° S is
429 observed, while more intense westerly winds are present in mid latitudes, revealing a anticyclonic
430 circulation, with the axis determining the line of change in wind speed. This pattern is well
431 defined during November, and the weakening westerlies are accompanied by positive values in
432 specific humidity in the same region of weakening westerly winds, even in northern latitudes
433 near to 10° S. The pattern in upper levels (Fig. 14) show a similar configuration with weakening
434 westerly winds during cases of early wet season onset during October, while in November, wind
435 configurations reveal a wide region of weakening northwesterly winds, which can be related with
436 an early southward migration and expansion of the Bolivian high.

437 *f. Trends in the wet season onset dates*

438 Results from the Mann-Kendall test reveal that groups 1 and 2 have experienced a delay in the
439 wet season onset since 1979 (Table 2). The first evaluation of this test, using the two-sided and one
440 sided Mann-Kendall test, expose a significance difference for these groups ($\alpha < 0.05$). With a
441 p-value of 0.0719 and 0.0285, groups 1 and 2 are significant at a 90 and 95% level, respectively.

442 Groups 3 and 4 do not reveal a significant trend in the onset dates in either the two-sided or the
443 one-sided Mann-Kendall test, despite p-values decrease. The Sens slope test ($\alpha < 0.05$) reveals
444 the magnitude of the trend in groups 1 and 2, which is 0.389 and 0.815 days per year, respectively.
445 Since 1979 group 1 has experienced a delay in onset dates of 0.4 days per year, while a higher delay
446 of 0.8 days per year has occurred in group 2. The Pettitt's test ($\alpha < 0.05$) reveal differences
447 in breaking points in the time series among the four groups. Particularly for groups 1 and 2, the
448 breaking point marks the year after which late cases of wet season onset become more frequent,
449 despite this test is only significant at a 90% level for group 1.

450 *g. Study cases: The very strong El Niño (1982-83) and the strong La Niña (1988-89)*

451 During El Niño year (Table 3), the wet season onset in each group occurs earlier than their
452 respective climatological onset date, with the beginning of the wet season taking place between
453 20 September and 11 November. Similarly, the wet season end occurs early, between 19 February
454 and 08 April. The wet season duration varies among the four groups. Group 4 present the longest
455 wet season whereas group 1 present the shortest wet season length. The analysis of the annual
456 and wet season precipitation reveals negative precipitation anomalies in both fields. Nevertheless,
457 a close analysis of the monthly precipitation (Table C1), reveals that between September and
458 November positive precipitation anomalies prevailed in the all groups, except, only for group 4
459 that present negative precipitation anomaly of 2.7 mm in October. During La Niña year, the wet
460 season onset in each group occur later than their climatological dates, between 30 November and
461 18 December (Table 4). The end of the wet season also occurs late in groups 1, 2, and 3 whereas
462 it occurs early in group 4. The wet season duration range from 124 days in the group 4 to 135
463 days in group 2. The annual and wet season precipitation in all groups were characterized by

464 negative precipitation anomalies. However, during October and November, negative precipitation
465 anomalies were common in the majority of the groups (Table C2).

466 **5. Discussion**

467 The main objective of this study was to determine the synoptic patterns related to wet season
468 timing in the tropical high Andes of southern Peru and Bolivia. Secondary objectives included
469 the examination of the interannual variability, including the comparison of cases of early vs late
470 wet season onset, the examination of trends on the wet season onset, and the analysis to ENSO
471 events (El Niño and La Niña). Results from this work reveals spatiotemporal differences in the
472 establishment of the wet season across the study area and a strong association between the wet
473 season onset and the duration of the wet season. In addition, we found that the gradual establish-
474 ment of the wet season onset was associated with the gradual transition to the summer atmospheric
475 features in South America. Across the study area groups 1 and 2, located southwest of the Titicaca
476 Lake, presented significant trends in the Mann-Kendall test, revealing that since 1979 they have
477 experienced a delay in the onset of the wet season in 0.4 and 0.8 days/year, respectively. More
478 study is necessary to assess the causes of these trends; however, a possible strength of westerly
479 winds in the middle and upper levels of the troposphere, associated with cases of late wet season
480 onset, can be related to these trends. In addition, cases of early and late wet season onset were
481 associated with changes in the position and strength of synoptic circulations in lower, middle,
482 and upper troposphere, that in turn are associated with the South American See-Saw. Finally, the
483 ENSO events analyzed showed an opposite behavior at the beginning of the wet season; however,
484 further analysis is needed to examine the main synoptic patterns at the very beginning of the wet
485 season during ENSO events.

486 *a. Seasonal cycle of precipitation*

487 This work uses a simple methodology based on the cumulative daily mean precipitation anomaly
488 to determine the exactly wet season timing across the tropical Andes of southern Peru and Bolivia.
489 The minimum and maximum point in the cumulative curve are tipping points associated with the
490 beginning and cessation of the wet season. These tipping points are reached when the daily mean
491 precipitation reaches the annual mean precipitation; this is, when the daily anomaly is zero or close
492 to zero. Our results reveal that along the study area, differences exists on the wet season timing,
493 particularly during the onset, where we found 37 days of difference between the onset in group 4
494 that occurs first and the onset in group 1 that occurs later. On the other hand, the end of the wet
495 season happens almost at the same time in all groups, which is reflected in a lower coefficient of
496 variation in each group. These variations range from 4.8 to 7.1% compared to the ones obtained for
497 the wet season onset that vary from 14.8 to 19.9%. These results are in agreement with Andrade
498 (2018) whom work revealed a two month period (October and November) for the establishment of
499 the wet season. Additionally, Ramallo (2013) found similar difference in days in the establishment
500 of the wet season between stations located in the proximity to Zongo valley (Bolivia) and stations
501 located over the Bolivian Altiplano. Moreover, the evolution of the mean daily precipitation in all
502 groups reveal a gradual increase in precipitation amount from the dry to the wet season, in a period
503 is called transition season in glaciological studies (Francou et al. 2003; Rabatel et al. 2013; Sicart
504 et al. 2011; Wagnon et al. 1999a,b). However, the transition from the wet to the dry season occurs
505 in a short period.

506 The high variability among the wet season onset can be associated with the apparent movement
507 of the sun and the latitudinal shift in the peak of insolation, in which solar rays strike perpen-
508 dicularly over the Earth surface (Garreaud et al. 2003). Atmospheric systems, such as the semi-

509 permanent high pressures, over the Pacific and Atlantic oceans, and wind belts in middle and upper
510 troposphere, follow this apparent movement, exhibiting a southward displacement from the June
511 (winter solstice) until December (summer solstice), and then shifting northward until March (fall
512 equinox). Therefore, there is more time to establish the wet season onset than there is to establish
513 the end of the wet season. The end dates do not reveal high variability because from March onward
514 solar rays will radiate most over the northern hemisphere, losing their influence over the tropics in
515 the southern hemisphere. Weather stations located in the north of the study area will experience
516 an early wet season onset. Indeed, the correlation analysis shows a strong relationship between
517 onset and latitude ($r = -0.61$), while longitude demonstrates a weaker relationship with the wet
518 season onset ($r = 0.27$). These correlations can be associated with a close proximity to the Ama-
519 zon basin, the main moisture source for precipitation events in the outer Andes (Perry et al. 2013,
520 2017). Results from the correlation matrix also reveal a strong relationship between the onset and
521 duration ($r = -0.97$). Moreover, since the end of the wet season does not reveal high variability
522 (lower CVs), we can conclude that the wet season length mostly depends on the wet season onset.
523 Similar results were achieved by Ramallo (2013) whom study found a strong significant relation-
524 ship between the wet season onset and the duration of the wet season after analyzed four different
525 methods to identify the rainy season in the Zongo valley.

526 *b. Synoptic patterns associated with wet season onset*

527 During the 37 days period, in which the wet season onset in established, the low-level north-
528 westerly flow east of the Andes showed a distinguished evolution. The progressively increase in
529 wind speed, over the Colombian, Peruvian, and northern Bolivian Jungle, is associated with the
530 southward displacement of the North Atlantic high-pressure that impulse the northeasterly Trade
531 winds toward South America (Nogués-Paegle and Mo 1997; Marengo et al. 2004). The develop-

532 ment of this low-level flux is related, as well to the presence of the South American Low-Level Jet
533 (SALLJ) during precipitation events in the outer Andes given its role transporting moisture from
534 the Amazon basin into the mountains (Lenters and Cook 1999; Vuille 1999; Perry et al. 2013,
535 2017; Guy et al. 2019; Chavez and Takahashi 2017). Different mechanisms have suggested the
536 relationship between the SALLJ and precipitation events in the Andes (Perry et al. 2013, 2017;
537 Junquas et al. 2017; Chavez and Takahashi 2017). Particularly, for the wet season onset, the
538 main feature is the increase in wind speed of this low-level flow, between the Colombian and
539 northern Bolivian jungle and the decrease in wind speed over Paraguay and northern Argentina.
540 Romatschke and Houze (2010) found a similar pattern, with a SALLJ restricted to the subtropics,
541 during deep convection events in the foothills of the central Andes. Nevertheless, we found that
542 the increase in wind speed of the SALLJ was gradual. Therefore, at the beginning of the wet sea-
543 son convective cores in the foothills of the central Andes and its associated stratiform precipitation
544 over the Andes (Chavez and Takahashi 2017; Romatschke and Houze 2010; Endries et al. 2018)
545 may not be the main mechanism that generates precipitation. Moisture influx through the valleys
546 and upslope winds, as a reaction to heating of the mountains and the Altiplano, would result in
547 the development of convective precipitation in the afternoon. However, more study is needed to
548 assess the spatiotemporal evolution of stratiform and convective precipitation in the outer tropical
549 Andes. This low-level configuration, in conjunction with the mid-troposphere anticyclonic circu-
550 lation and a southward displacement of westerlies in the subtropics favors the moisture transport
551 into areas located far from the Amazon basin. The anticyclonic circulation is also present during
552 wet episodes in the Andes, revealing, however, weak easterly winds and less moisture transport
553 during dry episodes (Vuille 1999). In addition, the low and middle level configuration can be
554 related to the development of the South Atlantic Convergence Zone (SACZ) associated with pre-
555 cipitation events in the study area (Lenters and Cook 1999; Vuille 1999; Guy et al. 2019) given

556 that a less intense low-level jet in the subtropics favors a northern shift of precipitation over an
557 extense area of tropical South America influence by SACZ (Nogués-Paegle and Mo 1997; Lieb-
558 mann et al. 2004; Carvalho et al. 2004). In upper levels of the troposphere, geopotential height
559 values reveal a vertical and horizontal expansion related with the establishment of Bolivian high.
560 Nevertheless, northwesterly winds prevail over easterly winds, associated with the Bolivian high,
561 above the Pacific Ocean and part of the western Andes Mountain. Since these northwesterly winds
562 demonstrate a trough configuration, divergence in this level seems to be not completely associated
563 with the Bolivian high but to the interaction of these two systems. Overall, the intensification of
564 the SALLJ in the northern and central part of the continent, the southward displacement of the
565 westerlies in the subtropics and the establishment of the Bolivian high have been describe as part
566 of the development phase of the South American Monsoon System (Zhou and Lau 2001).

567 *c. Seasonal cycle of atmospheric variables*

568 The analysis of the regimens of wind, specific humidity, and geopotential height reveals that
569 among these variables, tipping points associated with the onset and end of the wet season vary in
570 function of the latitude, longitude, and altitude in the troposphere. Of the two components of the
571 wind, its zonal component reveals a clear seasonality between 100 and 600 hPa. Despite tipping
572 points in high levels of the troposphere (400 to 100 hPa) are not directly associated with a changes
573 in wind direction, the detection of these tipping points, in average 10 days prior to the wet season
574 onset, reveals the importance of this wind component for the establishment of the wet season. On
575 the other hand, the evaluation of the meridional wind did not reveal a clear seasonality as the zonal
576 component in all levels analyzed. Tipping points associated with the wet season onset and end
577 were not identify in high levels of the troposphere over the study area; however, were identify
578 tipping points in lower and middle levels of the troposphere, between 925 to 400 hPa. In middle

579 levels, it was observed a decrease in southerly winds and the presence of northerly winds during
580 the period related to the wet season. In low levels, northerly winds prevails during the wet season;
581 however, this behavior was only found east to the Andes over the Peruvian jungle, and can be
582 closely related to the development of the low-level jet. We believe, that this seasonality has gone
583 unnoticed due to low values of wind speed in the areas compare to the high values over southeast
584 South America and due to established threshold used to identify the SALLJ. The specific humidity
585 seasonality is similar to the zonal wind patterns. In middle levels of the troposphere, tipping points
586 in this variable commonly occurs, in average, seven days after the occurrence of tipping point in
587 the zonal wind. This results, demonstrate the importance of zonal wind to transport moisture
588 from the Amazon basin into the high Andes. Nevertheless, mid-level moisture transport is not the
589 only mechanism in charge of increase moisture in the Andes. The low-level northwesterly flow is
590 another important mechanism, present during wet season episodes during the wet season, and, as
591 we mention before, for the begging of the wet season. The geopotential height seasonality in high
592 troposphere, reveal an indistinct pattern regarding its vertical evolution. However, the horizontal
593 evolution demonstrate a radial pattern. Overall, the change in seasonality of the geopotential
594 height in high levels occurs in a similar period to the establishment of the wet season onset. Thus,
595 the establishment of the Bolivian High occurs in conjunction with the development of the wet
596 season. This analysis reveals that zonal wind in middle and upper troposphere over the study
597 area is a good indicator to predict the wet season onset in the outer tropical Andes, as well as the
598 meridional wind, in mid-troposphere over the study region and in low-troposphere over the eastern
599 slope of the Andes, and specific humidity in mid troposphere over the study area.

600 *d. Early versus late wet season onset*

601 Cases of early and late wet season onset tend to occur indistinctly among groups in the study
602 area. Nevertheless, these cases present analogous characteristics. The majority of years that
603 present an early wet season onset have a longest wet season compared to their climatological
604 mean and to the cases of late wet season onset. Additionally, cases of early wet season onset were
605 more likely to present positive anomalies in the annual and wet season precipitation, while the
606 opposite behavior was observed in cases of late wet season onset. (Ramallo 2013) found similar
607 results in Zongo valley, where humid years were associated with a long wet season and dry years
608 with a short wet season. However, other variables such as the frequency and intensity of precipita-
609 tion among these cases need to be addressed in future studies; a particular case that deserves special
610 attention is the occurrence of late wet season onset and early wet season end due to its implica-
611 tions in water availability. These two scenarios (early and late wet season onset) do affect water
612 resources, as well as tropical glaciers. Despite cases of early wet season onset usually present
613 positive precipitation anomalies during the hydrologic year, principally, during the establishment
614 of the wet season, from October to November, anomalous dry periods were also present within the
615 wet season. These dry periods in the core of the wet season enhance melt rates due to low albedo,
616 mainly in the low surfaces of glaciers (Francou et al. 1995, 2003). On the other hand, late cases of
617 wet season onset revealed a more critical scenario because of the negative precipitation anomalies
618 and the extended dry periods in the wet season and in the transition season that characterized these
619 years. Hence, glacier melt rates occur in a longer period compared to cases of early wet season
620 onset. Furthermore, since positive precipitation anomalies are found in the majority of cases of
621 early wet season onset, as well as extended dry periods, it may be possible that heavy precipitation
622 events occur within the wet season during years characterized by an early wet season onset.

623 The analysis of the synoptic patterns revealed a slight intense (around $3-5 \text{ ms}^{-1}$) low-level north-
624 westerly over southern Bolivia and Paraguay during cases of early wet season onset compared to
625 the late cases of wet season onset. This wind intensification is associated with an increase in mois-
626 ture content between southern Peru and central Argentina in about 2 gkg^{-1} . A deeper low-pressure
627 over central-northern Argentina together with an intense high-pressure in the Atlantic Ocean are
628 responsible for the wind intensification, given that winds in the northern part of the continent did
629 not reveal high differences between the two scenarios evaluated. This low-level pattern is oppo-
630 site to what was found by Romatschke and Houze (2010) during deep convection episodes in the
631 foothills of the central Andes. Thus during cases of early wet season onset, deep convection may
632 be reduced in the foothills, and so the stratiform precipitation in the outer Andes. Convection due
633 to the heat of the Altiplano and surrounding mountains may be the main mechanism responsi-
634 ble for generating precipitation during cases of early wet season onset. In addition, a contrast in
635 moisture content is observed at a continental scale, with low values over the northern and central
636 part and high values in southeast South America. This dipole pattern, with a stronger SALLJ in
637 the subtropics than in the tropics is related to the one of the phases of the South American See-
638 Saw (Guy et al. 2019), associated with precipitation events in Cordillera Vilcanota and Cordillera
639 Real. the other phase, is determinate by an intense SACZ and a weak SALLJ over the subtropics.
640 (Carvalho et al. 2004) in a close analysis of the SACZ determined that intense precipitation on
641 north-northeastern Brazil is characterized by a phase of the MJO, in which the suppressed rainfall
642 is found over Indonesian and enhanced precipitation over the central Pacific: while the opposite
643 features were found during a decrease in rainfall in the same area. Thus, this continental-scale
644 See-Saw pattern may be closely related to the MJO, as (Nogués-Paegle and Mo 1997) suggested.
645 Meanwhile, in the middle troposphere, a pattern of weakening westerly winds between 15 and
646 25S was observed, which is clearer during November. This weakening is accompanied by posi-

647 tive values in specific humidity in the same region of weakening westerly winds. The presence
648 of weaker westerly winds during early wet season onsets would also reduce vertical wind shear,
649 favoring the development of convective clouds over the outer tropical Andes. Moreover, a trough
650 pattern off the coast of Chile in middle levels observed in groups 1, 3, and 4, during October can
651 induce the development the low-pressure over northern Argentina through the advection of vor-
652 ticity while crossing the Andes. Nevertheless, a close analysis even by even is needed, since the
653 monthly means can smooth atmospheric conditions. The pattern in upper levels shows a similar
654 configuration with weakening westerly winds during cases of early wet season onset during Oc-
655 tober, while in November, wind configuration reveals a wide region of weakening northwesterly
656 winds, which can be related with an early southward migration and expansion of the Bolivian
657 High.

658 *e. Trends in the wet season onset*

659 Significant trends were just found in two of the four groups analyzed, groups 1 and 2, at a 95%
660 significant level. These trends reveal a delay in about 0.4 and 0.8 days/year in these groups, re-
661 spectively. These results are in agreement with the occurrence of cases of early wet season onset,
662 which were more frequent in the 80s and 90s, while cases of late wet season onset were more com-
663 mon from late 90s in ahead. Nevertheless, since this work did not examine the relationship among
664 the wet season onset and wet season precipitation or frequency and intensity of precipitation, we
665 cannot conclude that this delay can be associated with a reduction of rainfall during the wet season
666 or other characteristics. These results reveal, however, that socioeconomic sectors such as agri-
667 culture, hydropower, mining, etc. can be affected in the following years if these trends continue,
668 endangering, as well water used for domestic consumption. Factors that may be responsible for
669 this trends need to be examined in future works, particularly changes in the mid and upper-level

670 zonal wind since our findings, as well as other researches, suggest a strong relationship between
671 this component of the wind and precipitation in the central Andes in all time scales (Garreaud et al.
672 2003; Andrade 2018). Moreover, the importance of the SALLJ for precipitation in the central An-
673 des point out the necessity to evaluate changes in the moisture transport into the central Andes, in
674 a context in which this system is becoming more intense in recent decades affecting, as well, the
675 hydrologic cycle over the Plata basin (Montini and Jones 2018). Furthermore, since many glacio-
676 logical studies report an exacerbating glacier retreat since the 1970s in the outer tropical Andes
677 (Rabatel et al. 2013; Salzmann et al. 2013), relating glacier shrinking with changes in the precip-
678 itation regimens, other variables need to be analyzed, given that no significant trends were found
679 in the onset dates in groups 3 and 4, the closest areas to the glaciers. Lastly, the increasing trend
680 in moisture in upper troposphere close to glaciers may play an important role in the exacerbated
681 glacier loss since slight and no significant trend in the total amount of precipitation was found
682 (Salzmann et al. 2013).

683 *f. Comparison between the very strong El Niño and the strong La Niña years*

684 The comparison between the two ENSO events reveal that the onset of the wet season has an
685 early occurrence during the very strong El Niño year and a late occurrence during the strong La
686 Niña. This in agreement with the positive and negative precipitation anomalies, respectively, found
687 during the months in which the wet season is established. The presence of negative precipitation
688 anomalies during the rest of the wet season were common in both cases. Nevertheless, largest
689 anomalies were found during the very strong El Niño. Just in April during the strong La Niña
690 positives anomalies prevailed, associated with the late occurrence of the wet season end. The
691 duration of the wet season is greater during El Niño than during La Niña year, except for group
692 1. Therefore, despite present an early wet season onset and long wet season, the very strong El

693 Niño years did not present positive precipitation anomalies as the majority of the cases analyzed
694 in section 4d, which present an early wet season onset, a long wet season, and positive precipita-
695 tion anomalies. Negative precipitation anomalies in the core of the wet season were presented in
696 both events affecting glaciers mass balance, as well as impacting on the socioeconomic activities
697 over the Altiplano (Andrade 2018; Vuille et al. 2018). Negative precipitation anomalies over the
698 Altiplano during the 1982-83 El Niño year have been associated with upper-level westerly wind
699 anomalies, which inhibited the moisture transport from the Amazon basin into the Andes, and
700 probably with the volcanic eruption of Chichón that caused a reduction of incoming shortwave
701 radiation over the Altiplano (Andrade 2018). However, at the beginning of the wet season, partic-
702 ularly in September and October, positive precipitation anomalies could be associated with winter
703 patterns, such as cut-off lows, frequent in the transition months from the dry to the wet season
704 (Vuille 1999; Garreaud et al. 2003).

705 **6. Conclusions**

706 This study improve the understanding on the establishment of the wet season in the outer tropical
707 Andes of South America. In this regions spatiotemporal differences in the wet season timing were
708 found, revealing an NW-SE orientation mostly associated with the distance to the equator and to
709 the Amazon basin. Among the wet season timing, the onset presents high variability, revealing 37
710 days of differences between its occurrences along groups located in the eastern and western side
711 of the study region. Moreover, the duration of the wet season is strongly influenced by the wet
712 season onset, given that the wet season end did not reveal high variability over the period analyzed.
713 A key factor in the establishment of the wet season is the southward displacement of the synoptic
714 system toward the austral summer and the proximity to the Amazon basin. In lower levels of the
715 troposphere, the evolution of the SALLJ plays an important role in transporting moisture from the

716 Amazon basin into the outer tropical Andes, particularly for regions located close to the Amazon
717 basin. While regions located near to the Pacific basin, moisture transport in mid-troposphere
718 from the southeast Amazon basin is relevant for the occurrence of the wet season onset. In the
719 upper troposphere, divergence during the establishment of the wet season is generated by the
720 interaction between a trough located over the Pacific ocean and the Bolivian high. In addition, a
721 close analysis of atmospheric variables reveals that the change in the seasonality of zonal wind in
722 the mid and upper troposphere, occurs in average 10 days prior to the establishment of wet season
723 onset in the group 1; likewise, the change in seasonally in specific humidity occurs in about 3
724 days after the change in the zonal wind. The comparison between early and late wet season onset
725 demonstrate that groups can present indistinctly cases of early or late wet season onset. In most of
726 the cases analysed, early (late) wet season onsets are related to positive (negative) annual and wet
727 season precipitation anomalies. At synoptic scale, an intense low-level northwesterly flow between
728 Bolivia and Argentina prevails during early wet season onset during October and November, as
729 well as weaker westerly and northwesterly winds in the mid and upper troposphere, respectively.
730 Statistically significant trends using the Mann-Kendall test were found in groups 1 and 2, revealing
731 that since 1979 these groups have experienced a delay in the wet season onset in 0.4 and 0.8 days
732 per year, respectively. Both ENSO events examined show an opposite behavior in the occurrence
733 of the wet season onset. Further analysis is needed to assess the causes of ongoing delay of the
734 wet season onset in the southwestern side of the study area, as well as, the synoptic circulations
735 related with wet and dry episodes at the beginning of the wet season during ENSO events. Finally,
736 results from this paper can be used to improve water management by local governments paying
737 special attention to the groups in which a delay of the wet season was found.

738 *Acknowledgments.* We would like to thank to the National Weather Services of Peru (SENAMHI
739 Peru) and Bolivia (SENAMHI Bolivia) as well as the DECADE Project for the data provided
740 to this study. This work was founded by the National Science Foundation Grant AGS-1347179
741 (CAREER: Multiscale Investigations of Tropical Andean Precipitation) to L.B. Perry. Special
742 thanks are also due to Dr. Anton Seimon, Heather Guy and Joseph Jonaitis for their important
743 contribution and advice to this work.

744 APPENDIX A

745 **Correlation Analysis**

746 APPENDIX B

747 **Cases of early and late wet season onset**

748 *a. Cases of early and late wet season onset in group 1 between 1979-80 and 2016-17 hydrologic*
749 *years*

750 *b. Cases of early and late wet season onset in group 2 between 1979-80 and 2016-17 hydrologic*
751 *years*

752 *c. Cases of early and late wet season onset in group 3 between 1979-80 and 2016-17 hydrologic*
753 *years*

754 *d. Cases of early and late wet season onset in group 4 between 1979-80 and 2016-17 hydrologic*
755 *years*

756 APPENDIX C

757 **Study cases El Niño 1982-83 and La Niña 1988-89**

758 *a. The very strong El Niño year (1982-83)*

759 *b. The strong La Niña year (1988-89)*

760 **References**

761 Andrade, M. F., 2018: *Atlas-clima y eventos extremos del Altiplano Central peru-boliviano / Cli-*
762 *mate and exrteme events from the Central Altiplano of Peru and Bolivia 1981-2010*. Geograph-
763 ica Bernensia, 188 pp., doi:10.4480/GB2018.N01.

764 Carvalho, L. M. V., C. Jones, and B. Liebmann, 2004: The south atlantic convergence zone: Inten-
765 sity, form, persistence, and relationships with intraseasonal to interannual activity and extreme
766 rainfall. *J. Climate*, **17**, 88–108.

767 Chavez, S. P., and K. Takahashi, 2017: Orographic rainfall hot spots in the andes-amazon transition
768 according to the trmm precipitation radar and insitu data. *J. Geophys. Res. Atmos.*, **122**, 5870–
769 5882, doi:10.1002/2016JD026282.

770 Danielson, J., and D. Gesch, 2011: Global multi-resolution terrain elevation data 2010
771 (gmted2010). Open-file repor, U.S. Geological Survey, 26 pp.

772 Dee, D. P., and Coauthors, 2011: The era-interim reanalysis: Conguration and performance of the
773 data assimilation system. *Q. J. R. Meteorol. Soc.*, **137**, 553–597.

774 Drenkhan, F., M. Carey, C. Huggel, J. Seidel, and M. T. Oré, 2015: The changing water cycle:
775 climatic and socioeconomic drivers of water-related changes in the andes of peru. *WIREs Water*,
776 **2**, 715733, doi:10.1002/wat2.1105.

- 777 Dunning, C. M., E. C. L. Black, and R. P. Allan, 2016: The onset and cessation of seasonal rainfall
778 over africa. *J. Geophys. Res. Atmos.*, **121** (11), 405424, doi:10.1002/2016JD025428.
- 779 Endries, J. L., and Coauthors, 2018: Radar-observed characteristics of precipitation in the tropical
780 high andes of southern peru and bolivia. *J. Appl. Meteor. Climatol.*, **57**, 1441–1458, doi:10.
781 1175/JAMC-D-17-0248.1.
- 782 Francou, B., P. Ribstein, R. Saravia, and E. Tiriau, 1995: Monthly balance and water discharge of
783 an inter-tropical glacier: Zongo glacier, cordillera real, bolivia, 16° S. *Journal of Glaciology*,
784 **41** (137), 61–67.
- 785 Francou, B., M. Vuille, P. Wagnon, J. Mendoza, and J.-E. Sicart, 2003: Tropical climate change
786 recorded by a glacier in the central andes during the last decades of the twentieth century:
787 Chacaltaya, bolivia, 16° S. *J. Geophys. Res.*, **108** (0), XXXX, doi:doi:10.1029/2002JD002959.
- 788 Garreaud, R., M. Vuille, and A. C. Clement, 2003: The climate of the altiplano: observed current
789 conditions and mechanisms of past changes. *Palaeogeography, Palaeoclimatology, Palaeoecol-*
790 *ogy*, **194**, 5–22, doi:10.1016/S0031-0182(03)00269-4.
- 791 Garreaud, R. D., and P. Aceituno, 2001: Interannual rainfall variability over the south american
792 altiplano. *J. Climate*, **14**, 2779–2789.
- 793 Garreaud, R. D., M. Vuille, R. Compagnucci, and J. Marengo, 2009: Present-day south ameri-
794 can climate. *Palaeogeography, Palaeoclimatology, Palaeoecology*, **281**, 180–195, doi:10.1016/
795 j.palaeo.2007.10.032.
- 796 Gilford, M. T., M. J. Vojtesak, G. Myles, R. C. Bonam, and D. L. Martens, 1991: South america
797 south of the amazon river—a climatological study. USAFETAC Tech. Note USAFETAC/TN–
798 92/004, USAFETAC, 716 pp.

- 799 Guy, H., A. Seimon, L. Perry, B. Konecky, M. Rado, M. Andrade, M. Potocki, and P. Mayewski,
800 2019: Subseasonal variations of stable isotopes in tropical andean precipitation. *Journal of*
801 *Hydrometeorology*, **23**, 3762–3791, under Review.
- 802 Hamed, K. H., and A. R. Raos, 1998: A modified mann-kendall trend test for autocorrelated data.
803 *Journal of Hydrology*, **204**, 182–196.
- 804 Hanshaw, M. N., and B. Bookhagen, 2014: Glacial areas, lake areas, and snow lines from 1975 to
805 2012: status of the cordillera vilcanota, including the quelccaya ice cap, northern central andes,
806 peru. *The Cryosphere*, **8**, 359–376, doi:10.5194/tc-8-359-2014.
- 807 Hunziker, S., S.Brnnimann, J. Calle, I. Moreno, M. Andrade, L. Ticona, A. Huerta, and W. Lavado-
808 Casimiro, 2018: Effects of undetected data quality issues on climatological analyses. *Climate*
809 *of the Past*, **14**, 1–20, doi:https://doi.org/10.5194/cp-14-1-2018.
- 810 Junquas, C., K. Takahashi, T. Condom, J.-C. Espinoza, S. Chavez, J. Sicart, and T. Lebel, 2017:
811 Understanding the influence of orography on the precipitation diurnal cycle and the associated
812 atmospheric processes in the central andes. *Clim Dyn*, doi:10.1007/s00382-017-3858-8.
- 813 Kaser, G., 2001: Glacier-climate interaction in low latitudes. *Journal of Glaciology*, **47 (157)**,
814 195–204.
- 815 Kronenberg, M., and Coauthors, 2016: The projected precipitation reduction over the central andes
816 may severely aect peruvian glaciers and hydropower production. *Energy Procedia*, **97**, 270–277.
- 817 Lenters, J. D., and K. H. Cook, 1995: On the origin of the bolivian high and related circulation
818 features of the south american climate. *J. Atmos. Sci.*, **54**, 656–677.
- 819 Lenters, J. D., and K. H. Cook, 1999: Summertime precipitation variability over south america:
820 role of the large-scale circulation. *Mon. Wea. Rev.*, **127**, 409–431.

821 Liebmann, B., S. Camargo, A. Seth, J. A. Marengo, L. Carvalho, D. Allured, R. Fu, and C. Vera,
822 2007: Onset and end of the rainy season in south america in observations and the echam 4.5
823 atmospheric general circulation model. *J. Climate*, **20**, 2037–2050, doi:10.1175/JCLI4122.1.

824 Liebmann, B., G. N. Kiladis, C. S. Vera, A. C. Saulo, and L. M. V. Carvalho, 2004: Subseasonal
825 variations of rainfall in south america in the vicinity of the low-level jet east of the andes and
826 comparison to those in the south atlantic convergence zone. *J. Climate*, **17**, 3829–3842, doi:
827 10.1175/JAMC-D-17-0248.1.

828 Liebmann, B., and J. A. Marengo, 2001: Interannual variability of the rainy season and aainfall in
829 the brazilian amazon basin. *J. Climate*, **14**, 4308–4318.

830 Marengo, J., W. R. Soares, C. Saulo, and M. Nicolini, 2004: Climatology of the low-level jet east
831 of the andes as derived from the ncepncar reanalyses: characteristics and temporal variability.
832 *J. Climate*, **17 (12)**, 2261–2280.

833 Montini, T., and C. Jones, 2018: Understanding linkages between the south american low-level jet
834 and large-scale circulation. *Fall Meeting 2018 AGU*, University of California Santa Barbara.

835 Nogués-Paegle, and K. C. Mo, 1997: Alternating wet and dry conditions over south america during
836 summer. *Mon. Wea. Rev.*, **125**, 279–290.

837 Perry, L. B., A. Seimon, and G. M. Kelly, 2013: Precipitation delivery in the tropical high andes
838 of southern peru: new ndings and paleoclimatic implications. *Int. J. Climatol*, doi:10.1002/joc.
839 3679.

840 Perry, L. B., and Coauthors, 2017: Characteristics of precipitating storms in glacierized tropical
841 andean cordilleras of peru and bolivia. *Annals of the American Association of Geographers*,
842 **107 (2)**, 309–322.

- 843 Pohlert, T., 2018: *trend: Non-Parametric Trend Tests and Change-Point Detection*. URL <https://CRAN.R-project.org/package=trend>, r package version 1.1.1.
- 844
- 845 Rabatel, A., and Coauthors, 2013: Current state of glaciers in the tropical Andes: a multi-century
846 perspective on glacier evolution and climate change. *The Cryosphere*, **7**, 81–102, doi:10.5194/
847 tc-7-81-2013.
- 848 Ramallo, C., 2013: Caractrisation du rgime pluviométrique et sa relation la fonte du glacier zongo
849 (cordillre royale). Ph.D. thesis, Sciences de la Terre, Universit Grenoble Alpes, Franais, 255
850 pp., nNT: 2013GRENU048. tel-01548283.
- 851 Romatschke, U., and R. A. Houze, Jr., 2010: Extreme summer convection in south america. *J.*
852 *Climate*, **23**, 3762–3791, doi:10.1175/2010JCLI3465.1.
- 853 Salzmann, N., C. Huggel, M. Rohrer, W. Silverio, B. G. Mark, P. Burns, and C. Portocarrero,
854 2013: Glacier changes and climate trends derived from multiple sources in the data scarce
855 cordillera vilcanota region, southern peruvian andes. *The Cryosphere*, **7**, 103–118, doi:10.5194/
856 tc-7-103-201.
- 857 Schauwecker, S., and Coauthors, 2017: The freezing level in the tropical andes, peru: an indicator
858 for present and future glacier extents. *J. Geophys. Res. Atmos*, **122**, 5172–5189, doi:10.1002/
859 2016JD025943.
- 860 Sicart, J. E., R. Hock, P. Ribstein, M. Litt, and E. Ramirez, 2011: Analysis of seasonal varia-
861 tions in mass balance and meltwater discharge of the tropical zongo glacier by application of a
862 distributed energy balance model. *J. Geophys. Res*, **116**, D13105, doi:10.1029/2010JD015105.

- 863 Vergara, W., A. M. Deeb, A. M. Valencia, R. S. Bradley, B. Francou, A. Zarzar, A. Grunwaldt, and
864 S. M. Haeussling, 2007: Economic impacts of rapid glacier retreat in the andes. *Eos*, **88** (25),
865 261–268.
- 866 Vuille, M., 1999: Atmospheric circulation over the bolivian altiplano during dry and wet periods
867 and extreme phases of the southern oscillation. *Int. J. Climatol.*, **19**, 1579–1600.
- 868 Vuille, M., and Coauthors, 2018: Rapid decline of snow and ice in the tropical andes impacts,
869 uncertainties and challenges ahead. *Eart-Science Reviews*, **176**, 195–213.
- 870 Wagnon, P., P. Ribstein, B. Francou, and J. E. Sircat, 2001: Anomalous heat and mass budget of
871 glacier zongo, bolivia, during the 1997/98 el nio year. *Journal of Glaciology*, **47** (157), 21–28.
- 872 Wagnon, P., P. Ribstein, G. Kaser, and P. Berton, 1999a: Annual cycle of energy balance of zongo
873 glacier, cordillera real, bolivia. *J. Geophys. Res*, **104** (D4), 3907–3923.
- 874 Wagnon, P., P. Ribstein, G. Kaser, and P. Berton, 1999b: Energy balance and runoff seasonality of
875 a bolivian glacier. global and planetary change. *Global and Planetary Change*, **22**, 49–58.
- 876 Yue, S., P. Pilon, and G. Cavadias, 2002: Power of the mann-kendall and spearman's rho tests for
877 detecting monotonic trends in hydrological series. *Journal of Hydrology*, **259**, 254–271.
- 878 Zhou, J., and M.-K. Lau, 2001: Anomalous heat and mass budget of glacier zongo, bolivia, during
879 the 1997/98 el nio year. *Int. J. Climatol*, **21**, 1623–1644, doi:10.1002/joc.700.

880 **LIST OF TABLES**

881 **Table A1.** Correlation matrix perform following Pearson method among climatological
882 wet season timing (onset, end, and duration) and geographic and topographic
883 characteristic of each particular weather stations. 42

884 **Table B1.** Years with an early and late wet season onset in group 1 (upper and bottom in
885 the table, respectively), showing the wet season timing, annual and wet season
886 precipitation (mm), percentage of wet season precipitation (%), and annual and
887 wet season precipitation anomalies (mm). 43

888 **Table B2.** Years with an early and late wet season onset in group 2 (upper and bottom in
889 the table, respectively), showing the wet season timing, annual and wet season
890 precipitation (mm), percentage of wet season precipitation (%), and annual and
891 wet season precipitation anomalies (mm). 44

892 **Table B3.** Years with an early and late wet season onset in group 2 (upper and bottom in
893 the table, respectively), showing the wet season timing, annual and wet season
894 precipitation (mm), percentage of wet season precipitation (%), and annual and
895 wet season precipitation anomalies (mm). 45

896 **Table B4.** Years with an early and late wet season onset in group 2 (upper and bottom in
897 the table, respectively), showing the wet season timing, annual and wet season
898 precipitation (mm), percentage of wet season precipitation (%), and annual and
899 wet season precipitation anomalies (mm). 46

900 **Table C1.** Monthly precipitation (mm) (above) and monthly precipitation anomaly (mm)
901 (below) during the very strong El Niño year (1982-83). 47

902 **Table C2.** Monthly precipitation (mm) (above) and monthly precipitation anomaly (mm)
903 (below) during the strong La Niña year (1988-89). 48

904 **Table 1.** Climatological wet season timing (onset, end, and duration), annual precipita-
905 tion (mm), total wet season precipitation (mm), the percentage of wet season
906 precipitation (%), and coefficient of variation (%) of the onset, end and duration
907 according to each group in the study area. 49

908 **Table 2.** Trend Analysis, showing results from the Mann Kendall, two-sided (*) and
909 one-sided- upward (**), Sens Slope and Pettitts test according to each group. . . . 50

910 **Table 3.** Wet season timing (onset, end, and duration) during the very strong El Niño
911 year (1982-83), annual and wet season precipitation amounts and anomalies
912 (mm) according to each group 51

913 **Table 4.** Wet season timing (onset, end, and duration) during the strong La Niña year
914 (1988-89), annual and wet season precipitation amounts and anomalies (mm)
915 according to each group 52

916 Table A1. Correlation matrix perform following Pearson method among climatological wet season timing
 917 (onset, end, and duration) and geographic and topographic characteristic of each particular weather stations.

	Elevation	Latitude	Longitude	Aspect	Slope	Onset	End	Duration
Elevation	1							
Latitude	-0.26	1						
Longitude	0.23	-0.86	1					
Aspect	0.16	-0.03	0.06	1				
Slope	-0.30	0.21	-0.10	0.20	1			
Onset	0.09	-0.61	0.27	-0.10	-0.17	1		
End	0.17	0.45	-0.46	-0.10	-0.13	-0.29	1	
Duration	-0.04	0.66	-0.36	0.07	0.12	-0.97	0.51	1

918

919

920

921

Table B1. Years with an early and late wet season onset in group 1 (upper and bottom in the table, respectively), showing the wet season timing, annual and wet season precipitation (mm), percentage of wet season precipitation (%), and annual and wet season precipitation anomalies (mm).

Year	Onset	End	Duration	Annual precipitation (mm)	We season precipitation (mm)	Percentage wet season precipitation (%)	Annual precipitation anomaly (mm)	Wet season precipitation anomaly (mm)
1984-85	07/10	25/04	201	637.9	602.5	94.5	145.1	225.9
1985-86	12/11	16/04	156	725.0	642.6	88.6	232.2	266.0
1987-88	12/10	08/04	179	552.7	475.2	86.0	59.9	98.5
1990-91	19/10	23/03	156	497.6	418.1	84.0	4.9	41.4
1992-93	13/11	27/03	135	459.5	378.1	82.3	-33.3	1.4
1996-97	07/11	29/03	143	600.7	533.9	88.9	107.9	157.3
1997-98	01/11	03/04	154	427.2	317.4	74.3	-65.6	-59.3
2009-10	12/11	05/03	114	514.6	403.9	78.5	21.9	27.2
1981-82	16/12	10/04	116	554.6	433.1	78.1	61.8	56.5
1988-89	18/12	21/04	125	429.1	358.4	83.5	-63.7	-18.2
1989-90	29/12	18/03	80	341.7	192.5	56.3	-151.1	-184.2
1991-92	25/12	07/03	73	302.2	210.5	69.7	-190.6	-166.1
1999-00	23/12	12/03	80	466.3	341.1	73.1	-26.5	-35.6
2003-04	18/12	04/04	108	408.7	361.8	88.5	-84.1	-14.8
2006-07	15/12	02/04	109	426.3	314.3	73.7	-66.5	-62.4
2015-16	17/12	13/03	87	412.5	239.2	58.0	-80.3	-137.5
2016-17	26/12	04/04	100	462.1	337.4	73.0	-30.7	-39.2

922

923
924
925

Table B2. Years with an early and late wet season onset in group 2 (upper and bottom in the table, respectively), showing the wet season timing, annual and wet season precipitation (mm), percentage of wet season precipitation (%), and annual and wet season precipitation anomalies (mm).

Year	Onset	End	Duration	Annual precipitation (mm)	We season precipitation (mm)	Percentage wet season precipitation (%)	Annual precipitation anomaly (mm)	Wet season precipitation anomaly (mm)
1979-80	02/10	01/04	182	684.8	644.2	94.1	-2.9	106.7
1982-83	20/09	18/03	180	549.1	421.0	76.7	-138.6	-116.5
1984-85	03/10	27/04	207	1111.7	1023.0	92.0	423.9	485.5
1985-86	25/10	27/04	185	1171.2	1067.5	91.1	483.5	530.0
1987-88	12/10	12/04	183	754.7	656.9	87.0	67.0	119.4
1990-91	18/10	26/03	160	711.5	585.9	82.3	23.8	48.4
1996-97	06/10	17/04	163	740.5	669.7	90.4	52.8	132.2
1988-89	14/12	28/04	136	582.6	458.5	78.7	-105.1	-79.0
1989-90	12/12	18/02	69	570.4	287.1	50.3	-117.3	-250.4
1991-92	24/12	06/03	73	413.8	268.9	65.0	-273.9	-268.6
1997-98	19/12	02/04	105	581.4	358.3	61.6	-106.3	-179.2
1999-00	23/12	14/03	82	624.6	413.9	66.3	-63.1	-123.6
2004-05	13/12	05/04	114	567.3	426.7	75.2	-120.4	-110.8
2014-15	12/12	24/04	134	678.3	511.0	75.3	-9.4	-26.5
2015-16	18/12	13/03	86	582.7	338.1	58.0	-105.0	-199.4

926

927

928

929

Table B3. Years with an early and late wet season onset in group 2 (upper and bottom in the table, respectively), showing the wet season timing, annual and wet season precipitation (mm), percentage of wet season precipitation (%), and annual and wet season precipitation anomalies (mm).

Year	Onset	End	Duration	Annual precipitation (mm)	We season precipitation (mm)	Percentage wet season precipitation (%)	Annual precipitation anomaly (mm)	Wet season precipitation anomaly (mm)
1979-80	02/10	01/04	182	653.1	606.0	92.8	-40.5	65.5
1982-83	13/10	16/03	155	553.4	412.9	74.6	-140.2	-127.6
1984-85	11/10	25/04	197	934.8	863.6	92.4	241.2	323.1
1990-91	09/10	27/03	170	709.9	587.4	82.7	16.3	46.9
1993-94	02/10	27/04	208	784.6	717.3	91.4	91.1	176.8
1997-98	25/09	02/04	190	665.4	615.1	92.4	-28.2	74.6
2000-01	08/10	27/03	171	823.4	727.8	88.4	129.9	187.3
2002-03	01/10	05/04	187	868.0	766.2	88.3	174.4	225.7
2005-06	02/10	06/04	187	687.1	639.5	93.1	-6.4	99.0
1980-81	06/12	14/04	130	785.9	582.1	74.1	92.4	41.6
1986-87	05/12	23/03	109	671.7	457.0	68.0	-21.8	-83.6
1988-89	15/12	21/04	128	535.2	421.2	78.7	-158.3	-119.3
1989-90	23/12	18/03	86	559.3	324.3	58.0	-134.3	-216.3
1999-00	20/12	18/03	89	633.6	414.3	65.4	-60.0	-126.2
2001-02	06/12	23/04	139	728.7	555.9	76.3	35.2	15.4
2003-04	12/12	01/04	111	710.0	546.9	77.0	16.5	6.4
2004-05	09/12	07/04	120	600.1	441.7	73.6	-93.5	-98.8
2008-09	01/12	26/03	116	576.4	441.0	76.5	-117.2	-99.5
2010-11	04/12	02/04	120	585.7	488.4	83.4	-107.8	-52.1

930

931

932

933

Table B4. Years with an early and late wet season onset in group 2 (upper and bottom in the table, respectively), showing the wet season timing, annual and wet season precipitation (mm), percentage of wet season precipitation (%), and annual and wet season precipitation anomalies (mm).

Year	Onset	End	Duration	Annual precipitation (mm)	We season precipitation (mm)	Percentage wet season precipitation (%)	Annual precipitation anomaly (mm)	Wet season precipitation anomaly (mm)
1981-82	16/10	10/04	177	797.4	690.1	86.5	129.9	130.7
1982-83	14/10	08/04	177	556.5	468.6	84.2	-111.1	-90.8
1984-85	11/10	25/04	197	871.5	790.2	90.7	203.9	230.8
1987-88	16/10	14/04	181	773.4	693.2	89.6	105.9	133.8
1994-95	12/10	30/03	170	635.3	574.6	90.5	-32.3	15.2
1998-99	18/10	05/04	170	596.0	519.6	87.2	-71.6	-39.8
2000-01	11/10	28/03	169	756.8	655.9	86.7	89.2	96.5
2002-03	04/10	12/04	191	830.4	745.0	89.7	162.8	185.6
2013-14	12/10	28/03	168	674.0	586.2	87.0	76.4	26.8
1980-81	07/12	12/04	127	757.9	576.0	76.0	90.4	16.6
1988-89	30/11	02/04	124	602.0	481.8	80.0	-65.6	-77.6
1989-90	14/12	18/03	95	544.4	311.1	57.1	-123.2	-248.3
1999-00	06/12	14/03	99	575.6	389.9	67.7	-92.0	-169.5
2003-04	09/12	29/03	111	677.7	480.8	70.9	10.1	-78.6
2004-05	09/12	03/04	116	587.2	418.0	71.2	-80.3	-141.4
2010-11	04/12	08/04	126	607.6	503.9	82.9	-60.0	-55.5
2011-12	09/12	02/04	115	644.7	439.8	68.2	-22.8	-119.6
2014-15	08/12	16/04	130	660.1	481.3	72.9	-7.4	-78.1

934

935 Table C1. Monthly precipitation (mm) (above) and monthly precipitation anomaly (mm) (below) during the
 936 very strong El Niño year (1982-83).

Group	Jul	Aug	Sep	Oct	Nov	Dec	Jan	Feb	Mar	Apr	May	Jun
1	1.2	1.6	28.9	36.2	54.1	23.7	42.8	52.1	22.9	24.6	3.6	1.5
2	2.7	3.5	63.8	78.0	88.9	44.9	58.3	65.1	60.6	53.4	21.7	8.2
3	0.8	12.0	46.3	70.8	105.6	57.7	77.8	67.1	50.9	45.8	14.1	4.5
4	0.8	7.9	35.7	47.3	116.5	62.1	80.4	82.3	58.1	51.6	9.5	4.3
1	-3.1	-7.1	14.5	11.9	20.0	-49.6	-79.6	-44.7	-52.3	-3.1	-2.5	-3.9
2	-3.4	-8.4	39.4	35.6	36.7	-54.0	-97.9	-59.4	-45.9	8.4	10.0	0.5
3	-3.5	0.4	22.8	20.1	42.7	-51.8	-70.1	-51.1	-51.1	-0.9	4.2	-1.8
4	-3.6	-1.9	13.6	-2.7	51.0	-40.3	-60.2	-28.3	-42.1	5.2	-0.6	-1.3

937

938 Table C2. Monthly precipitation (mm) (above) and monthly precipitation anomaly (mm) (below) during the
 939 strong La Niña year (1988-89).

Group	Jul	Aug	Sep	Oct	Nov	Dec	Jan	Feb	Mar	Apr	May	Jun
1	1.7	0.7	14.8	19.1	7.3	55.3	95.7	86.7	91.5	47.0	5.1	4.1
2	4.6	1.6	29.0	29.2	20.8	89.4	137.5	87.8	90.5	74.1	12.3	5.7
3	0.6	0.0	13.0	41.3	13.2	100.9	128.4	78.3	76.8	67.9	9.8	5.2
4	0.0	0.5	7.4	40.6	21.3	104.9	135.6	105.3	121.2	49.3	8.2	7.8
1	-2.6	-7.9	0.4	-5.3	-26.8	-18.0	-26.8	-10.1	16.4	19.3	-1.0	-1.3
2	-1.5	-10.3	4.5	-13.2	-31.4	-9.5	-18.6	-36.7	-16.0	29.1	0.6	-2.0
3	-3.8	-11.6	-10.5	-9.4	-49.8	-8.7	-19.5	-39.9	-25.2	21.2	-0.1	-1.1
4	-4.4	-9.3	-14.8	-9.4	-44.1	2.6	-4.9	-5.3	21.0	2.8	-1.9	2.1

940

941 TABLE 1. Climatological wet season timing (onset, end, and duration), annual precipitation (mm), total wet
 942 season precipitation (mm), the percentage of wet season precipitation (%), and coefficient of variation (%) of
 943 the onset, end and duration according to each group in the study area.

Group	Onset	End	Duration	Annual	Wet season	Percentage	Coefficient of variation (%)		
				Precipitation (mm)	precipitation (mm)	wet season precipitation (%)	Onset	End	duration
1	30/11	05/04	127	492.8	376.7	76.4	14.8	7.1	26.3
2	13/11	07/04	146	687.7	537.5	78.2	17.1	6.6	24.8
3	12/11	08/04	148	693.5	540.5	77.9	19.9	5.3	20.6
4	24/11	11/04	170	667.5	559.4	83.8	16.3	4.8	18.7

944 TABLE 2. Trend Analysis, showing results from the Mann Kendall, two-sided (*) and one-sided- upward (**),
 945 Sens Slope and Pettitts test according to each group.

Group	Mann Kendall				Sen's slope			Pettitt's			
	tau	S	Var	p-value	p-value	slope	95% confidence interval	p-value	Change point	Kt	p-value
1	0.206	144	6314.667	0.0719	0.0360	0.389	-0.037-1.333	0.0719	1998-99	168	0.0989
2	0.251	175	6313.000	0.0285	0.0143	0.815	0.067-1.688	0.0285	1987-88	155	0.1547
3	0.043	30	6321.333	0.7153	0.3576	0.212	-0.714-1.000	0.7153	2002-03	68	1.2220
4	0.138	96	6312.667	0.1378	0.1159	0.357	-0.278-1.133	0.2318	2002-03	147	0.2001

946 TABLE 3. Wet season timing (onset, end, and duration) during the very strong El Niño year (1982-83), annual
 947 and wet season precipitation amounts and anomalies (mm) according to each group

Group	Onset	End	Duration	Annual precipitation (mm)	Annual precipitation anomaly (mm)	Wet season precipitation (mm)	Wet season precipitation anomaly (mm)
1	16/11	19/02	96	293.3	-199.5	155.4	-221.3
2	20/09	18/03	153	549.1	-138.6	421.0	-116.5
3	13/10	16/03	155	553.4	-140.2	410.5	-130.1
4	14/10	08/04	177	556.5	-111.1	468.6	-90.8

948 TABLE 4. Wet season timing (onset, end, and duration) during the strong La Niña year (1988-89), annual and
 949 wet season precipitation amounts and anomalies (mm) according to each group

Group	Onset	End	Duration	Annual precipitation (mm)	Annual precipitation anomaly (mm)	Wet season precipitation (mm)	Wet season precipitation anomaly (mm)
1	18/12	21/04	125	429.1	-63.7	358.4	-18.2
2	14/12	28/04	135	582.6	-105.1	458.5	-79.0
3	15/12	21/04	128	535.2	-158.3	411.0	-129.5
4	30/11	02/04	124	602.0	-65.6	481.8	-77.6

950 **LIST OF FIGURES**

951 **Fig. 1.** Study area showing the location of the 43 weather stations (black dots) located above 2500 m
 952 asl, with more than 90% completeness of precipitation observations and currently operating,
 953 and the surrounding cordilleras. 55

954 **Fig. 2.** Spatial distribution of the four subregions, cumulative daily mean precipitation anomaly (red
 955 line) and daily mean precipitation (blue bars) in each group. The minimum and maximum
 956 points in the red line mark the onset and end dates of the wet season. 56

957 **Fig. 3.** Temporal progression of the atmospheric conditions in lower (850 hPa), middle (500 hPa)
 958 and upper (200 hPa) levels of the troposphere for the onset dates in group 4 (a, b, c), group
 959 2 (d, e, f), and group 1 (g, h, i). 57

960 **Fig. 4.** The seasonal cycle of the zonal wind (ms^{-1}) in upper (a) and middle (b) levels of the tro-
 961 posphere averaged for the area between 18 and 12° S and 72.75 and 66.75° W. Black lines
 962 show the cumulative mean daily anomaly of this variable from 100 to 700 hPa. Colored
 963 lines represent the climatological mean daily values of the zonal wind. The pink rectangle
 964 marks the period in which wet season onset and end is established in all groups. 58

965 **Fig. 5.** The seasonal cycle of the meridional wind (ms^{-1}) in upper (a) and middle (b) levels of the
 966 troposphere averaged for the area between 18 and 12° S and 72.75 and 66.75° W. Black lines
 967 show the cumulative mean daily anomaly of this variable from 100 to 700 hPa. Colored lines
 968 represent the climatological mean daily values of the meridional wind. The pink rectangle
 969 marks the period in which wet season onset and end is established in all groups. 59

970 **Fig. 6.** The seasonal cycle of the specific humidity (gkg^{-1}) in upper (a) and middle (b) levels of the
 971 troposphere averaged for the area between 18 and 12° S and 72.75 and 66.75° W. Black lines
 972 show the cumulative mean daily anomaly of this variable from 100 to 700 hPa. Colored lines
 973 represent the climatological mean daily values of the specific humidity. The pink rectangle
 974 marks the period in which wet season onset and end is established in all groups. 60

975 **Fig. 7.** The seasonal cycle of the geopotential height ($gpdm$) in upper (a) and middle (b) levels of
 976 the troposphere averaged for the area between 18 and 12° S and 72.75 and 66.75° W. Black
 977 lines show the cumulative mean daily anomaly of this variable from 100 to 700 hPa. Colored
 978 lines represent the climatological anomaly daily values of the geopotential height. The pink
 979 rectangle marks the period in which wet season onset and end is establishment in all groups. 61

980 **Fig. 8.** Mean daily precipitation (mm) and mean daily precipitation anomaly (mm) during early (a
 981 and c) and late (b and d) wet season onset cases in group 1. 62

982 **Fig. 9.** Mean daily precipitation (mm) and mean daily precipitation anomaly (mm) during early (a
 983 and c) and late (b and d) wet season onset cases in group 2. 63

984 **Fig. 10.** Mean daily precipitation (mm) and mean daily precipitation anomaly (mm) during early (a
 985 and c) and late (b and d) wet season onset cases in group 3. 64

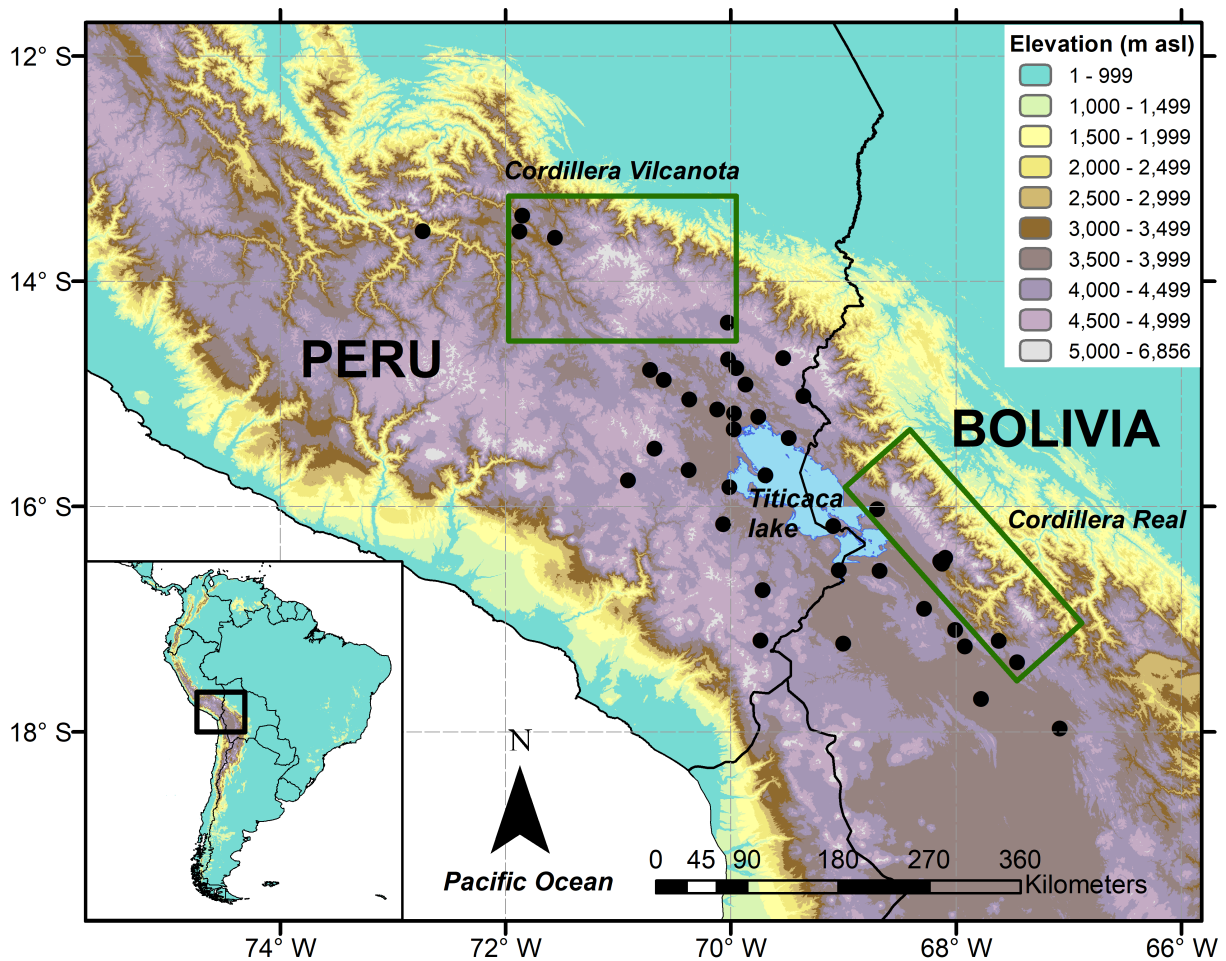
986 **Fig. 11.** Mean daily precipitation (mm) and mean daily precipitation anomaly (mm) during early (a
 987 and c) and late (b and d) wet season onset cases in group 4. 65

988 **Fig. 12.** Monthly differences in 850 hPa between early and late wet season onset among the four
 989 groups 1 (a and b), 2 (c and d), 3 (e and f), and 4 (g and h) in October (left panels) and
 990 November (right panels). Wind in vectors (ms^{-1}), specific humidity in shaded (gkg^{-1}),

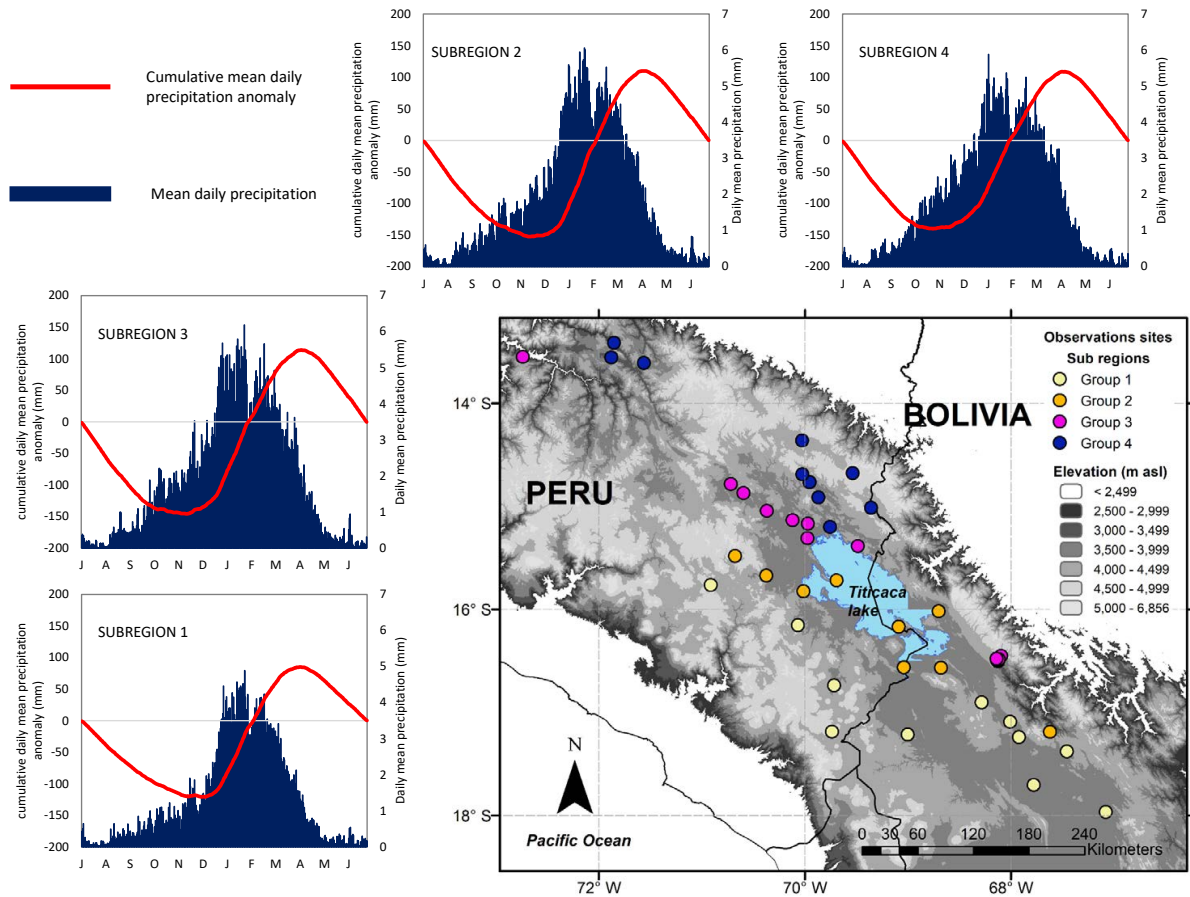
991 and geopotential height in contour (*gpdm*) with solid line showing positive differences and
992 dotted lines, negative differences. 66

993 **Fig. 13.** Monthly differences in 500 hPa between early and late wet season onset among the four
994 groups 1 (a and b), 2 (c and d), 3 (e and f), and 4 (g and h) in October (left panels) and
995 November (right panels). Wind in vectors (ms^{-1}), specific humidity in shaded (gkg^{-1}),
996 and geopotential height in contour (*gpdm*) with solid line showing positive differences and
997 dotted lines, negative differences. 67

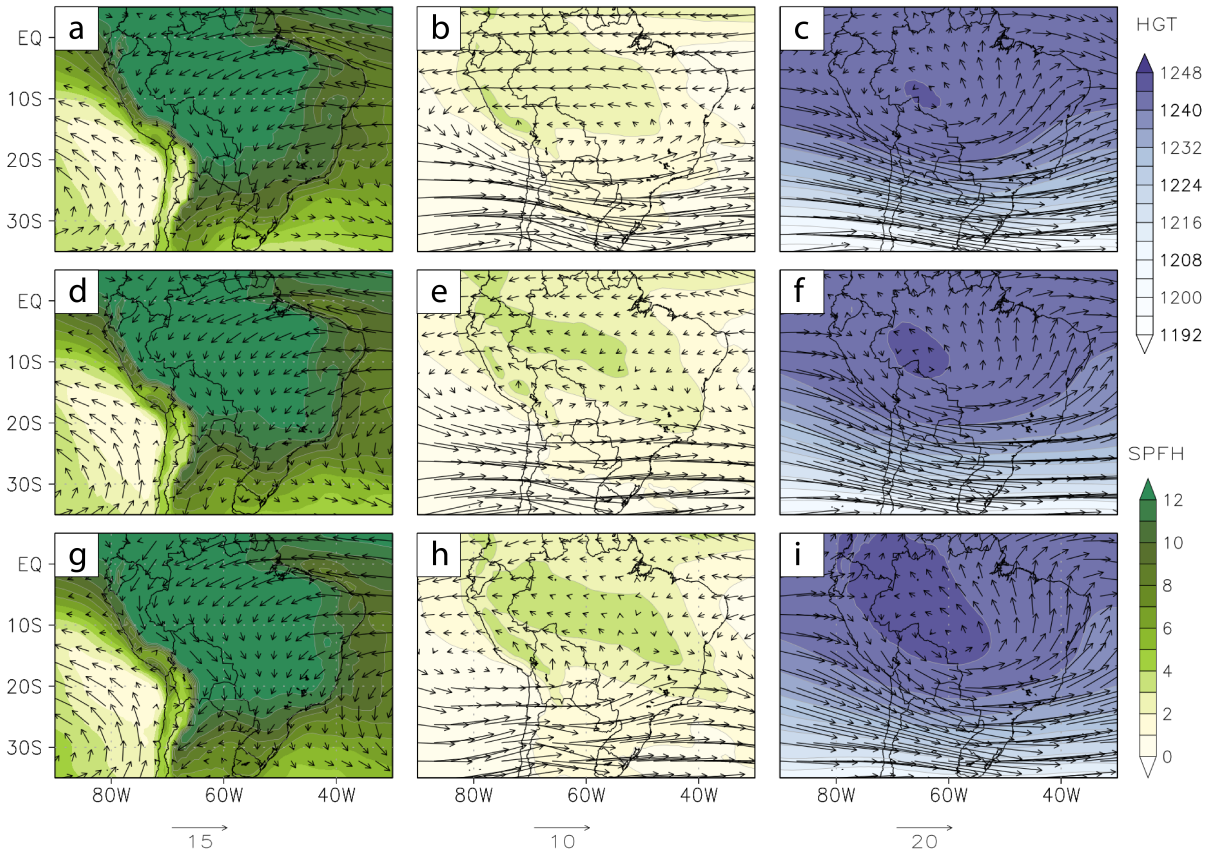
998 **Fig. 14.** Monthly differences in 200 hPa between early and late wet season onset among the four
999 groups 1 (a nad b), 2 (c and d), 3 (e and f), and 4 (g and h) in October (left panels) and
1000 November (right panels). Wind in vectors (ms^{-1}) and geopotential height in shaded (*gpdm*). . . 68



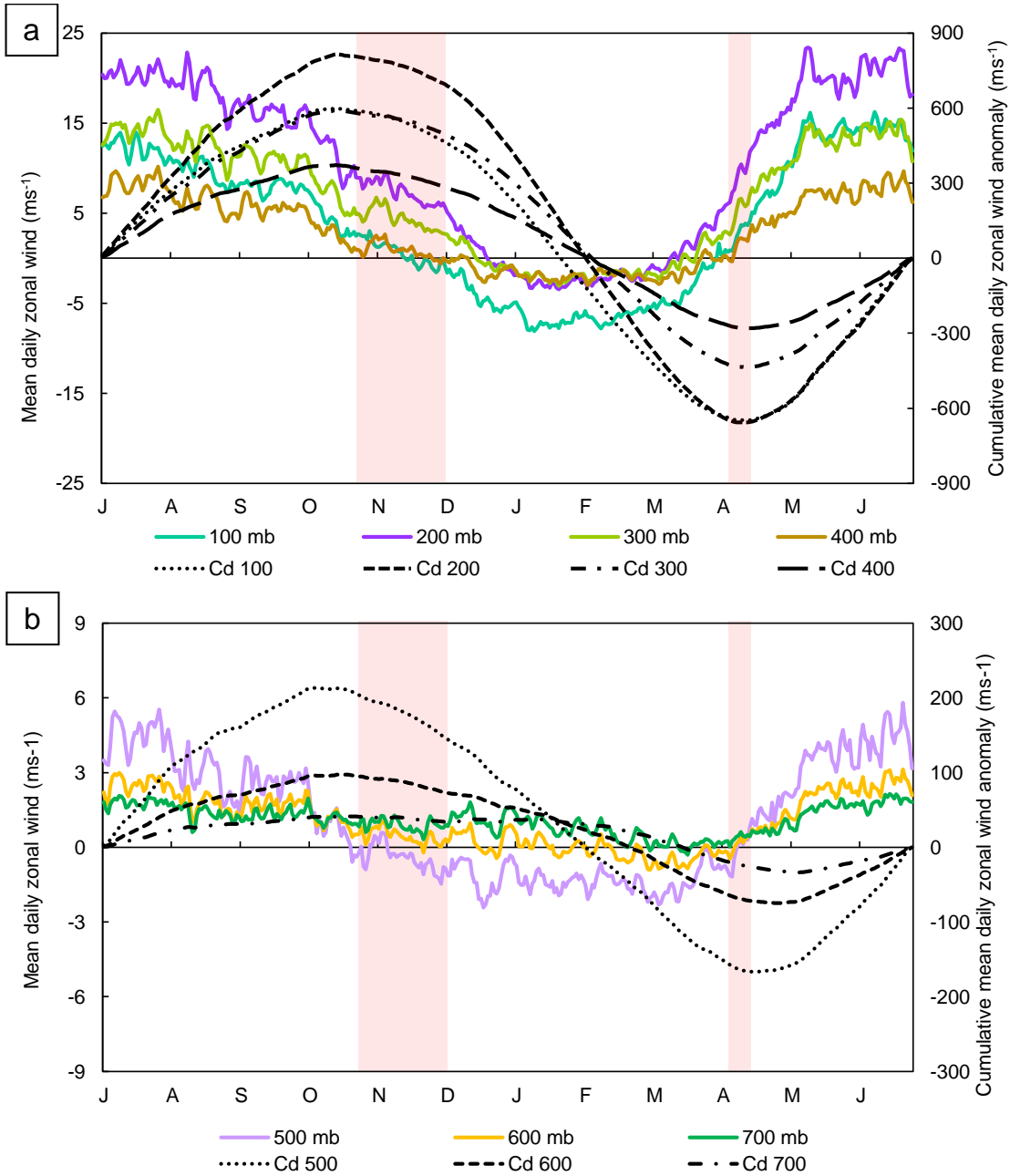
1001 FIG. 1. Study area showing the location of the 43 weather stations (black dots) located above 2500 m asl,
 1002 with more than 90% completeness of precipitation observations and currently operating, and the surrounding
 1003 cordilleras.



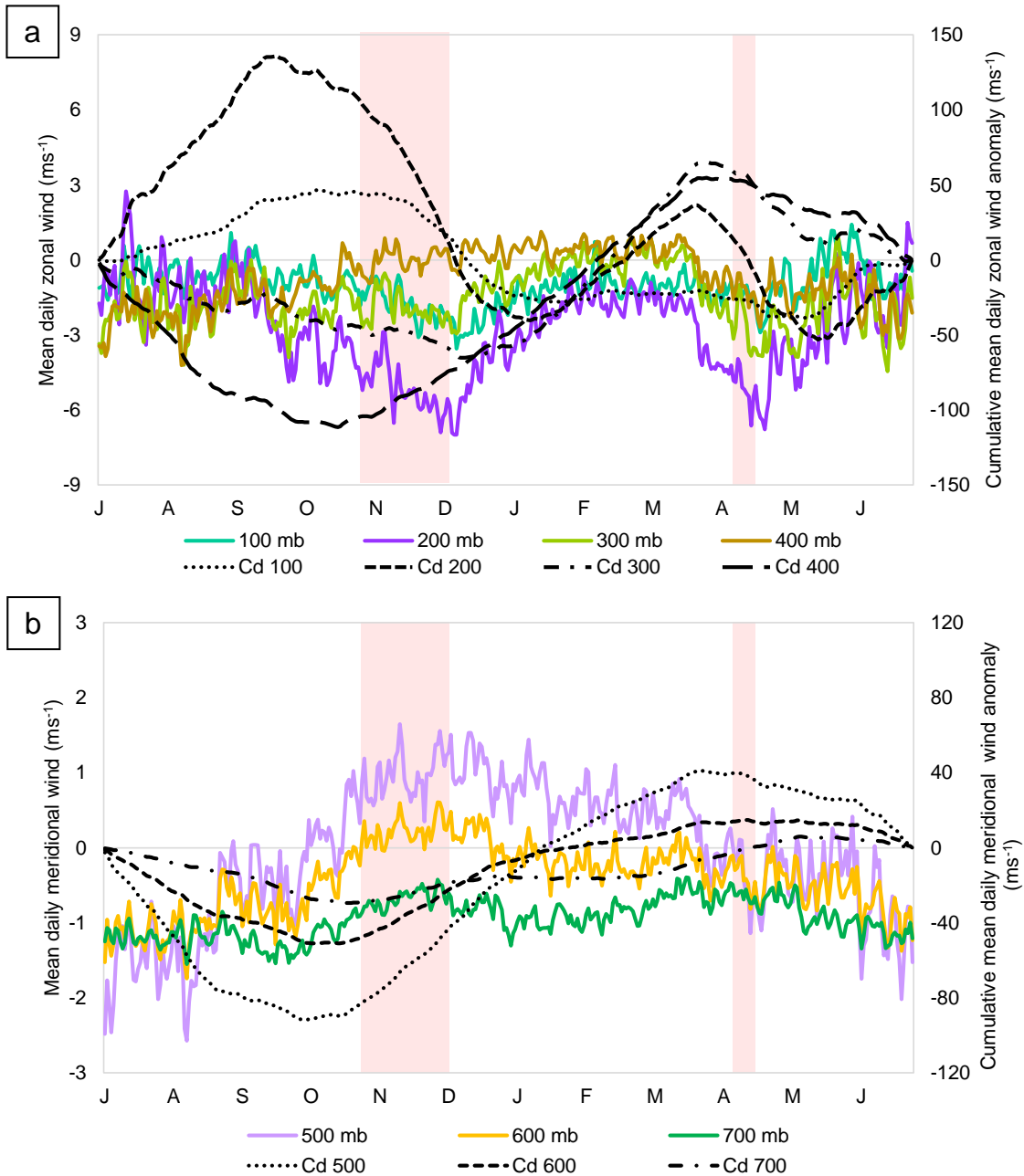
1004 FIG. 2. Spatial distribution of the four subregions, cumulative daily mean precipitation anomaly (red line) and
 1005 daily mean precipitation (blue bars) in each group. The minimum and maximum points in the red line mark the
 1006 onset and end dates of the wet season.



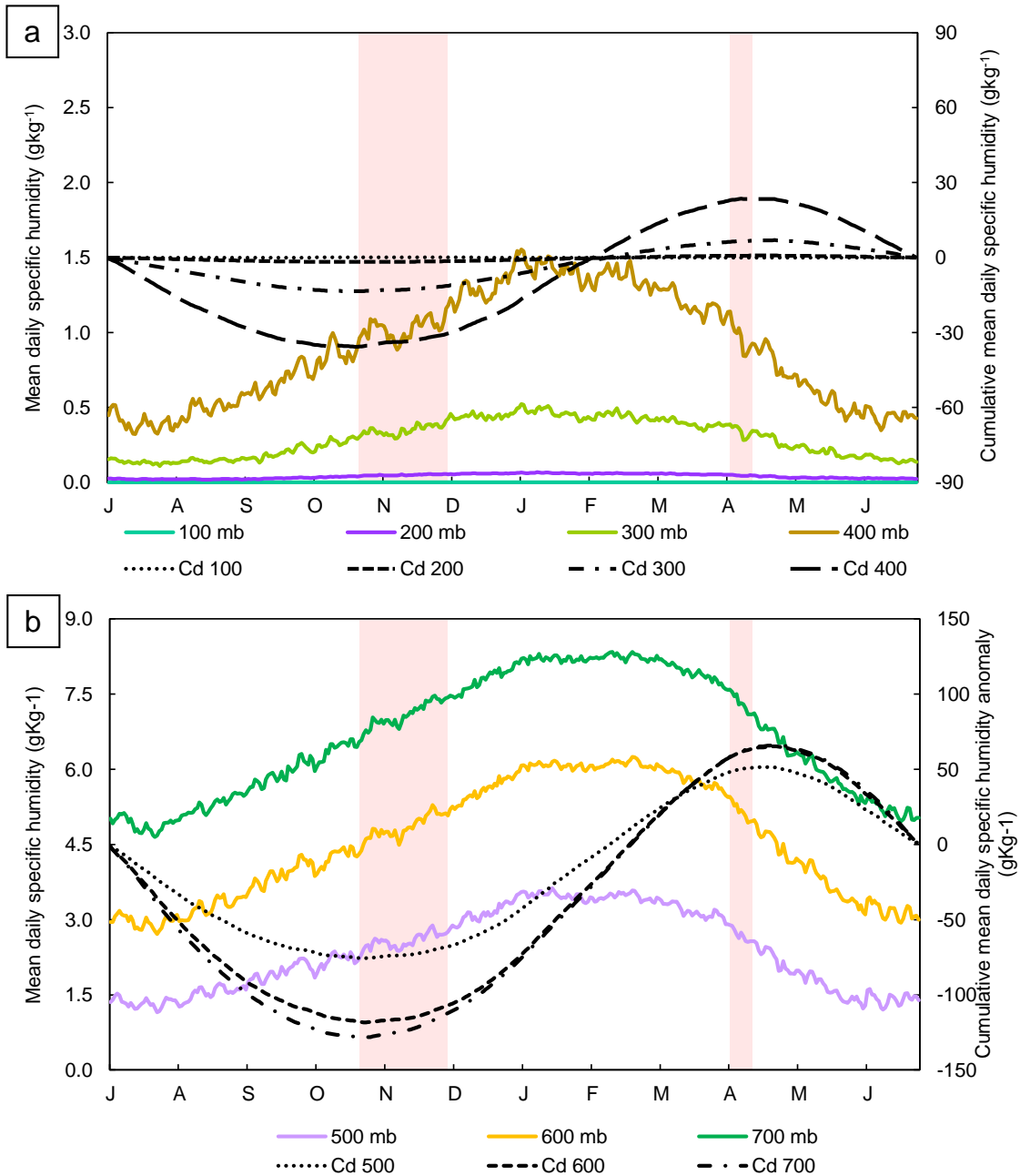
1007 FIG. 3. Temporal progression of the atmospheric conditions in lower (850 hPa), middle (500 hPa) and upper
 1008 (200 hPa) levels of the troposphere for the onset dates in group 4 (a, b, c), group 2 (d, e, f), and group 1 (g, h, i).



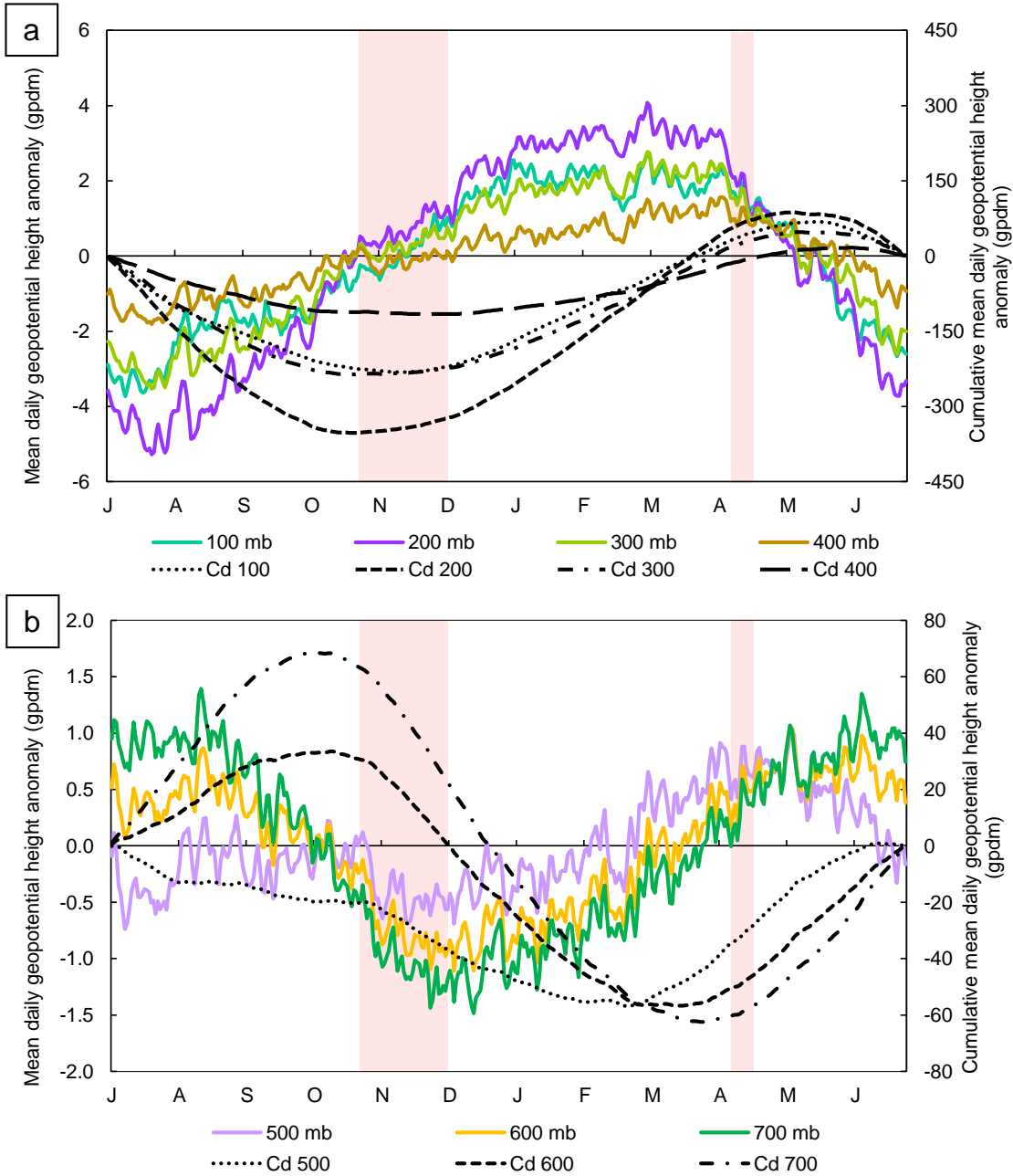
1009 FIG. 4. The seasonal cycle of the zonal wind (ms^{-1}) in upper (a) and middle (b) levels of the troposphere
 1010 averaged for the area between 18 and 12° S and 72.75 and 66.75° W. Black lines show the cumulative mean daily
 1011 anomaly of this variable from 100 to 700 hPa. Colored lines represent the climatological mean daily values of
 1012 the zonal wind. The pink rectangle marks the period in which wet season onset and end is established in all
 1013 groups.



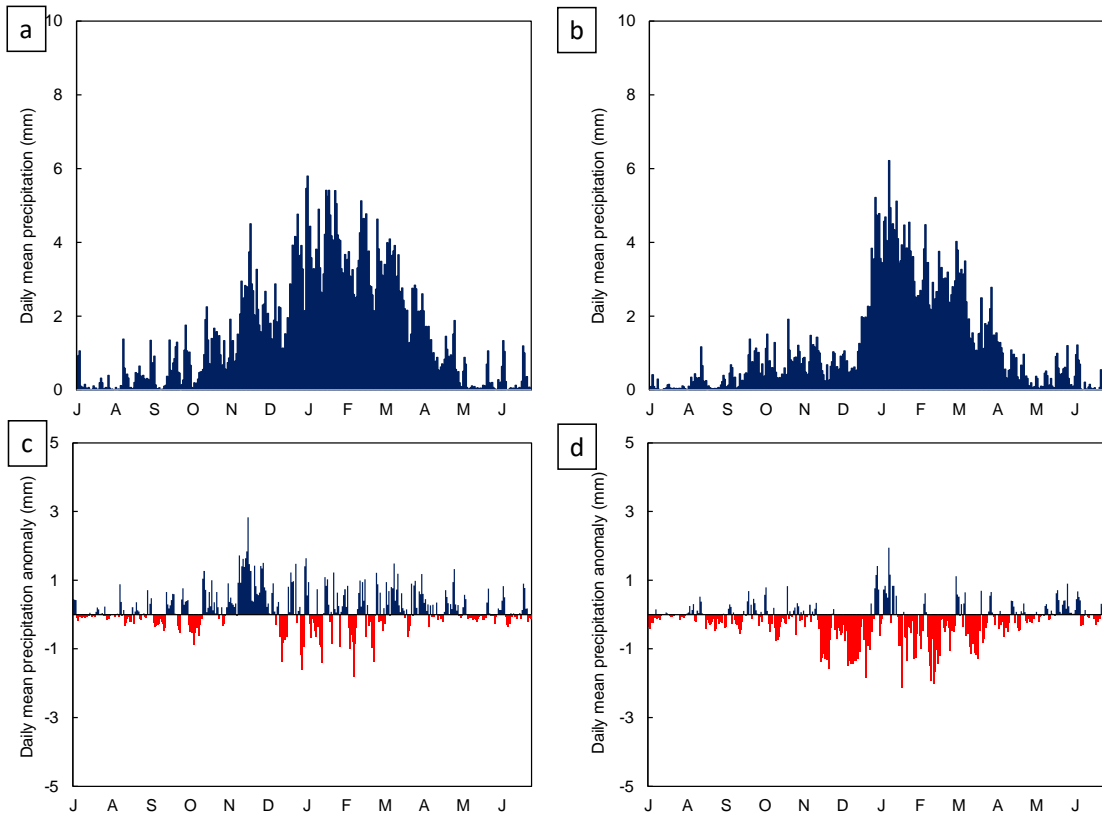
1014 FIG. 5. The seasonal cycle of the meridional wind (ms^{-1}) in upper (a) and middle (b) levels of the troposphere
 1015 averaged for the area between 18 and 12° S and 72.75 and 66.75° W. Black lines show the cumulative mean daily
 1016 anomaly of this variable from 100 to 700 hPa. Colored lines represent the climatological mean daily values of
 1017 the meridional wind. The pink rectangle marks the period in which wet season onset and end is established in
 1018 all groups.



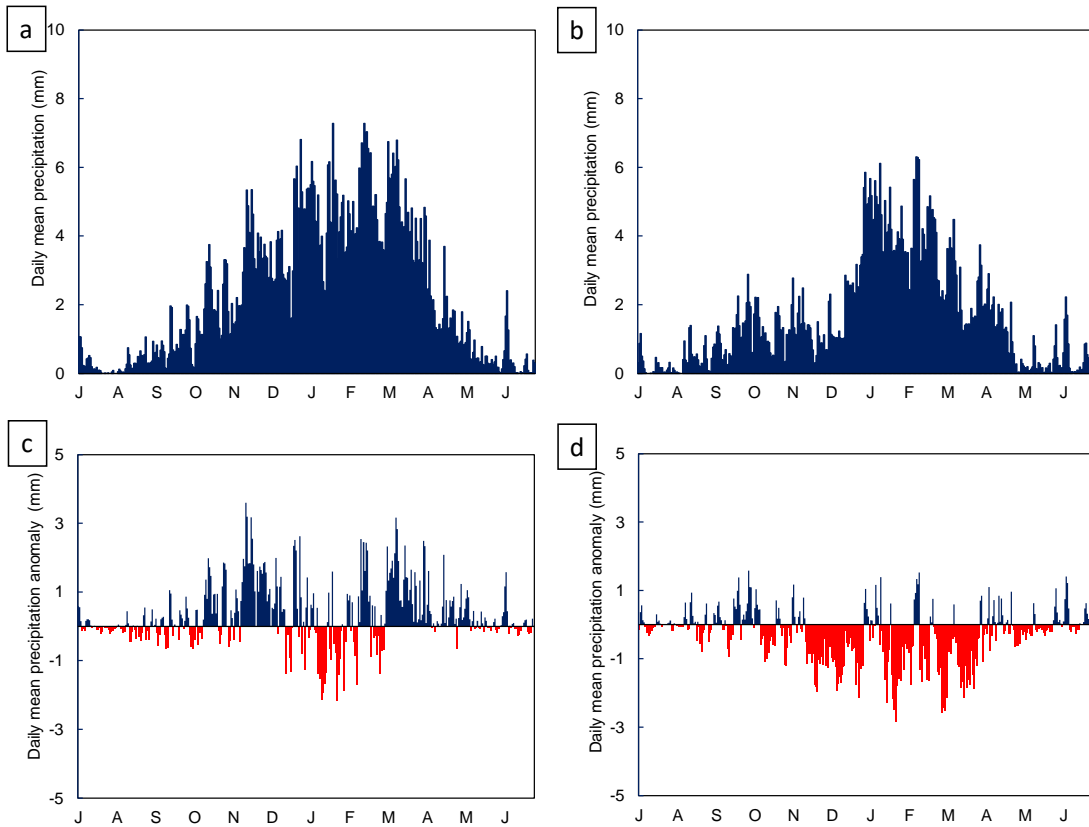
1019 FIG. 6. The seasonal cycle of the specific humidity (gkg^{-1}) in upper (a) and middle (b) levels of the tropo-
 1020 sphere averaged for the area between 18 and 12° S and 72.75 and 66.75° W. Black lines show the cumulative
 1021 mean daily anomaly of this variable from 100 to 700 hPa. Colored lines represent the climatological mean
 1022 daily values of the specific humidity. The pink rectangle marks the period in which wet season onset and end is
 1023 established in all groups.



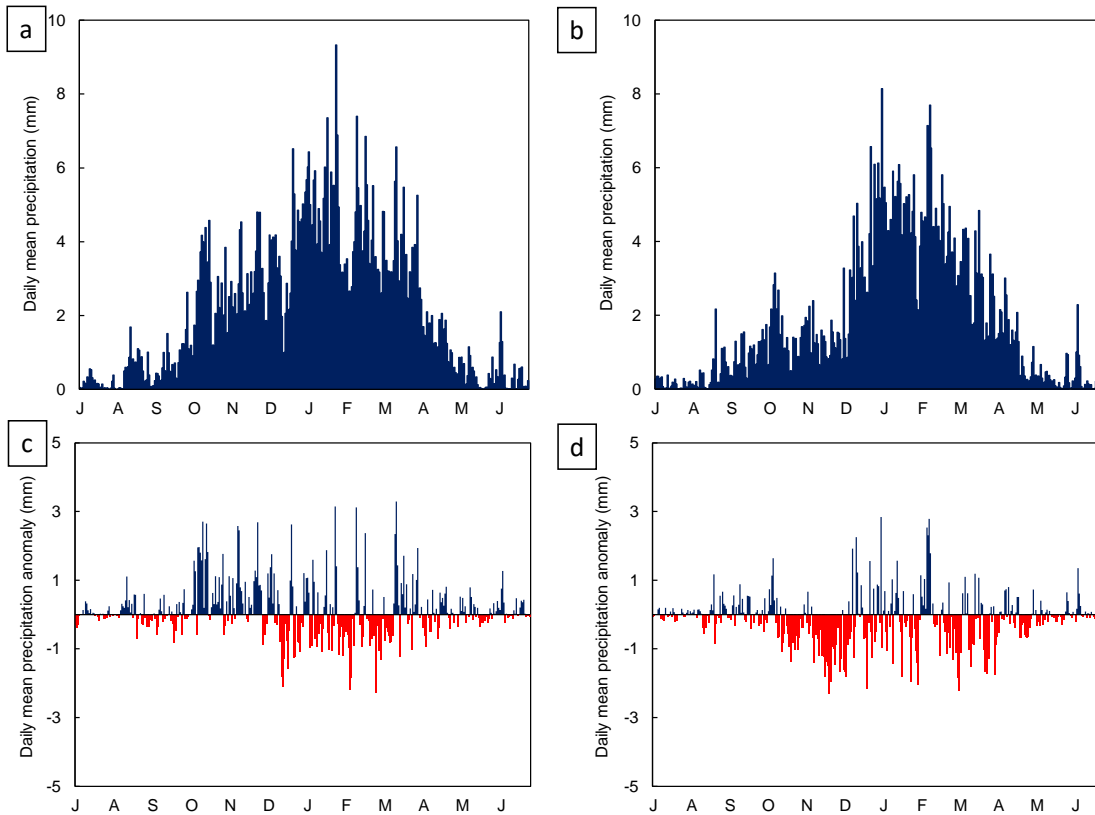
1024 FIG. 7. The seasonal cycle of the geopotential height (*gpdm*) in upper (a) and middle (b) levels of the
 1025 troposphere averaged for the area between 18 and 12° S and 72.75 and 66.75° W. Black lines show the cumulative
 1026 mean daily anomaly of this variable from 100 to 700 hPa. Colored lines represent the climatological anomaly
 1027 daily values of the geopotential height. The pink rectangle marks the period in which wet season onset and end
 1028 is establishment in all groups.



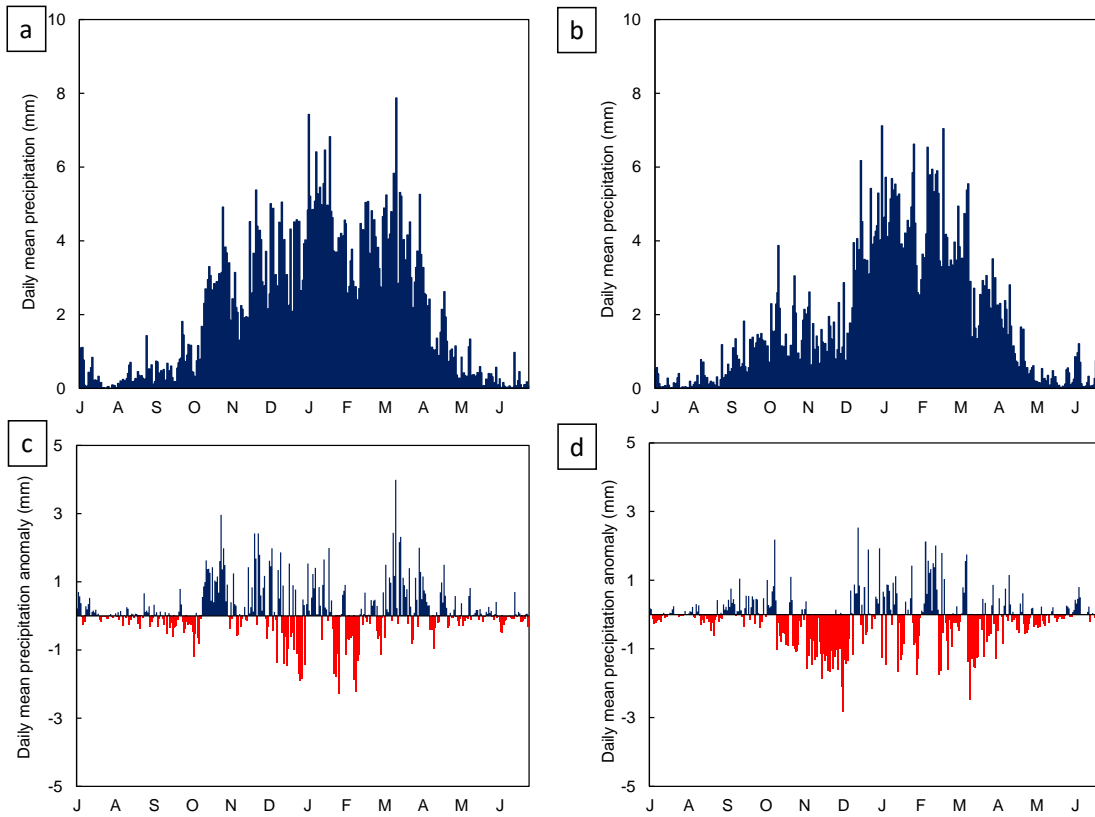
1029 FIG. 8. Mean daily precipitation (mm) and mean daily precipitation anomaly (mm) during early (a and c) and
 1030 late (b and d) wet season onset cases in group 1.



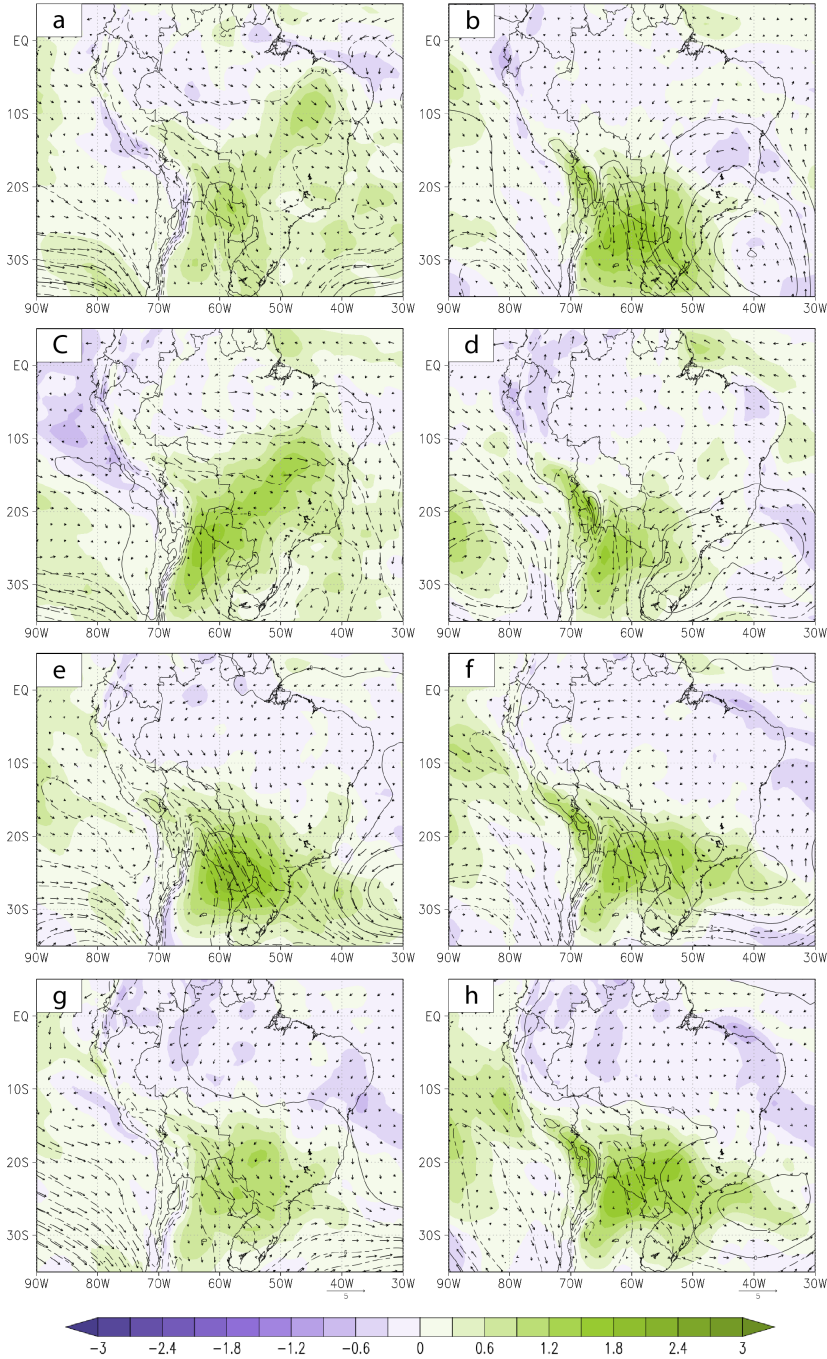
1031 FIG. 9. Mean daily precipitation (mm) and mean daily precipitation anomaly (mm) during early (a and c) and
 1032 late (b and d) wet season onset cases in group 2.



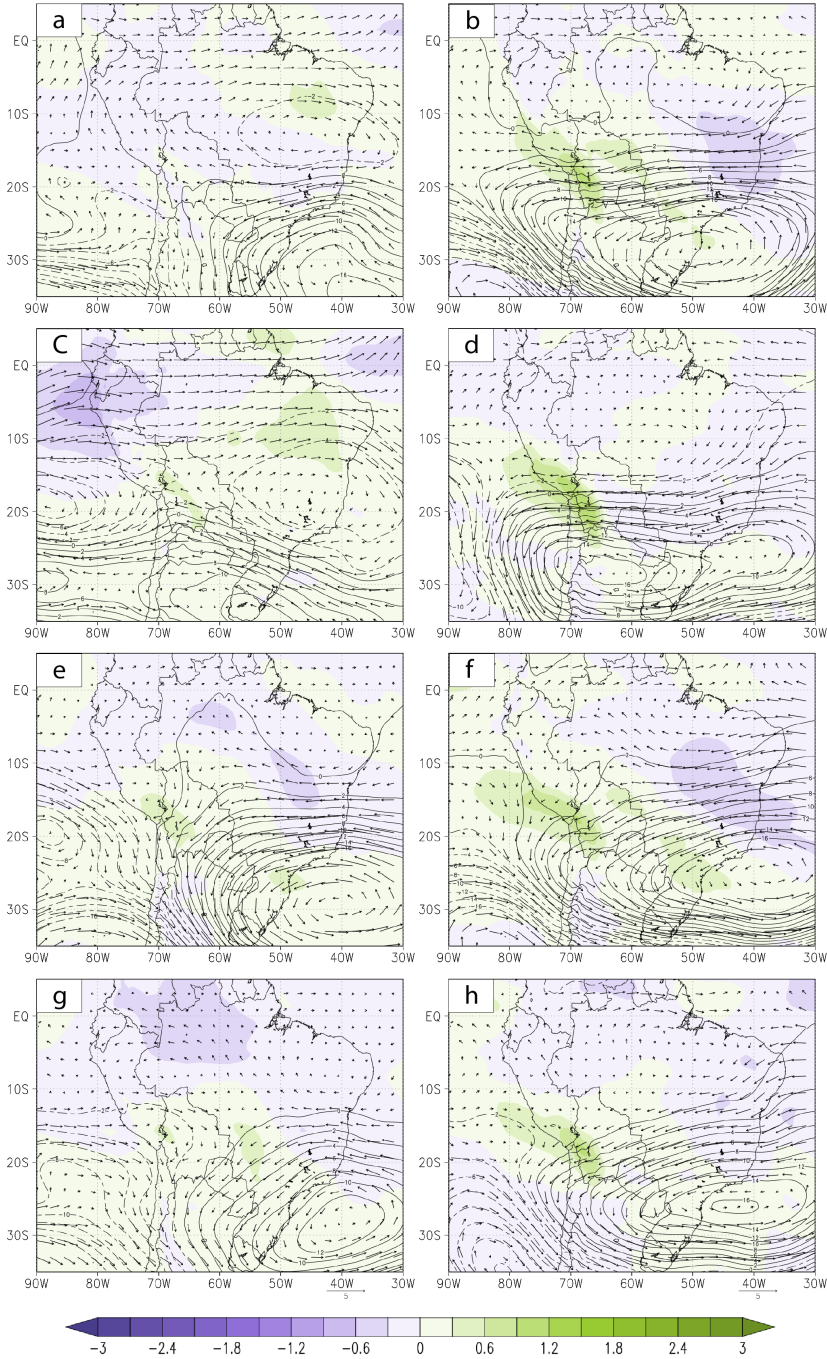
1033 FIG. 10. Mean daily precipitation (mm) and mean daily precipitation anomaly (mm) during early (a and c)
 1034 and late (b and d) wet season onset cases in group 3.



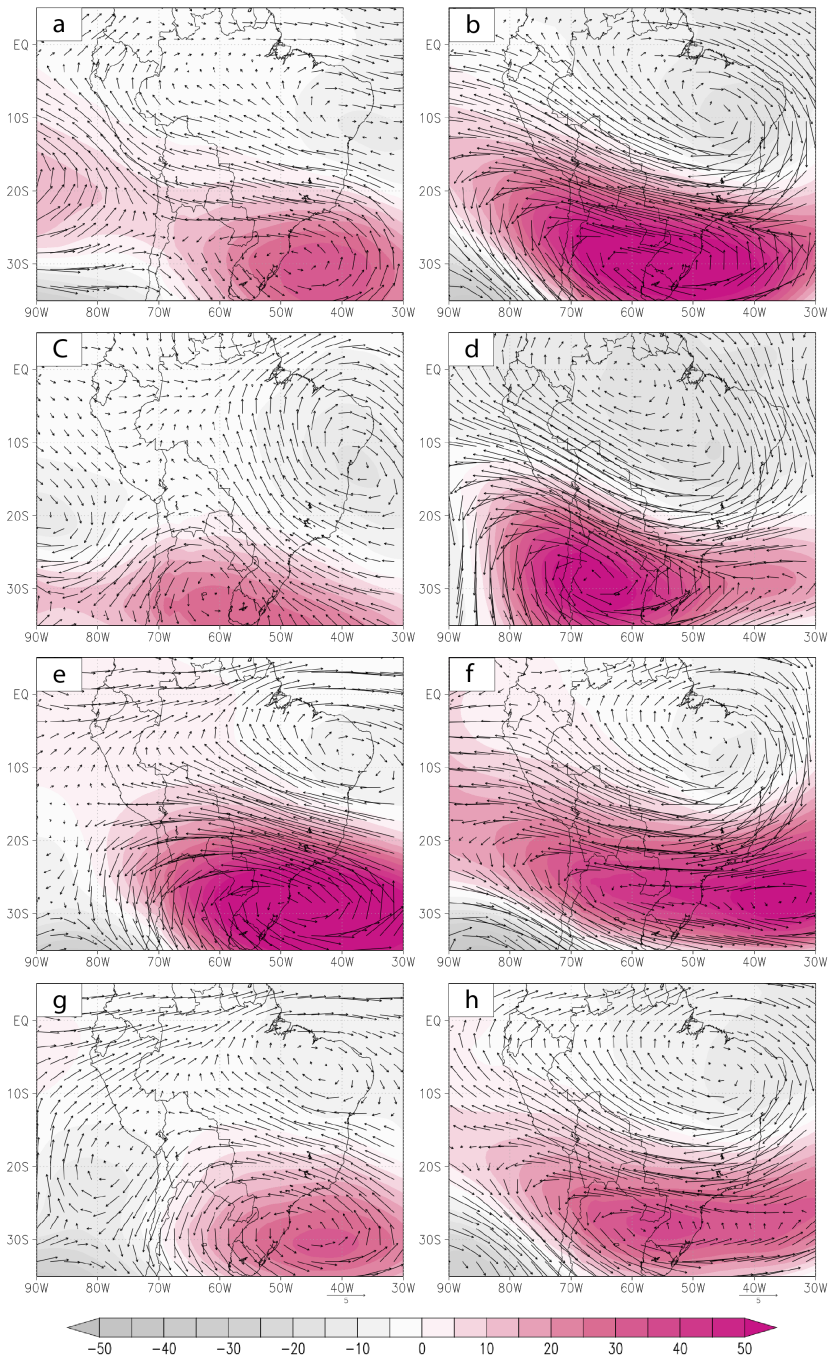
1035 FIG. 11. Mean daily precipitation (mm) and mean daily precipitation anomaly (mm) during early (a and c)
 1036 and late (b and d) wet season onset cases in group 4.



1037 FIG. 12. Monthly differences in 850 hPa between early and late wet season onset among the four groups 1 (a
 1038 and b), 2 (c and d), 3 (e and f), and 4 (g and h) in October (left panels) and November (right panels). Wind in
 1039 vectors (ms^{-1}), specific humidity in shaded (gkg^{-1}), and geopotential height in contour ($gpdm$) with solid line
 1040 showing positive differences and dotted lines, negative differences.



1041 FIG. 13. Monthly differences in 500 hPa between early and late wet season onset among the four groups 1 (a
 1042 and b), 2 (c and d), 3 (e and f), and 4 (g and h) in October (left panels) and November (right panels). Wind in
 1043 vectors (ms^{-1}), specific humidity in shaded (gkg^{-1}), and geopotential height in contour ($gpdm$) with solid line
 1044 showing positive differences and dotted lines, negative differences.



1045 FIG. 14. Monthly differences in 200 hPa between early and late wet season onset among the four groups 1 (a
 1046 nad b), 2 (c and d), 3 (e and f), and 4 (g and h) in October (left panels) and November (right panels). Wind in
 1047 vectors (ms^{-1}) and geopotential height in shaded ($gpdm$).

Vita

Tania K. Ita Vargas was born and raised in Carhuaz, a little town located in Cordillera Blanca in the northern Peruvian Mountains. After graduating from high school in 2005 and begging a career in Management, she moved to Lima to study Meteorology at the Agrarian National University, eventually graduating with honors in April of 2013. Soon After, Tania joined the SENAMHI Peru where she work for 5 years. During that time, she had the opportunity to attend the International Desk Meteorology at NOAA in College Park, Maryland, USA, where she was trained in weather forecast in South America. Tania moved to Boone, NC, in January 2018 to work as a graduate research assistant with Dr. Baker Perry at Appalachian State University to improve her understanding of precipitation in the tropical high Andes of Peru and its implications for tropical glaciers. As part of this work, she has had the opportunity to return to Peru for summer course and fieldwork in one occasion, gaining valuable experience in mountaineering and interacting closer with Andean partners of Dr. Perry.

After graduation with a M.A. in Geography in May 2019, Tania plans to return to Peru to continue study the weather and climate of the Andes. She also hope to work in deep with Andean communities in weather and climate forecasting, for which she also plan to study Quechua as soon as come back to Peru.